Modern Aspects of Liquid Metal Engineering

FRANK CZERWINSKI

Liquid metal engineering (LME) refers to a variety of physical and/or chemical treatments of molten metals aimed at influencing their solidification characteristics. Although the fundamentals have been known for decades, only recent progress in understanding solidification mechanisms has renewed an interest in opportunities this technique creates for an improvement of castings. This review covers conventional and novel concepts of LME with their application to modern manufacturing techniques based not only on liquid but also on semisolid routes. The role of external forces applied to the melt combined with grain nucleation control is explained along with laboratory- and commercial-scale equipment designed for implementation of various concepts exploring mechanical, electromagnetic, and ultrasound principles. An influence of melt treatments on quality of the final product is considered through distinguishing between internal integrity of net shape components and the alloy microstructure. Recent global developments indicate that exploring the synergy of melt chemistry and physical treatments achieved through LME allows creating the optimum conditions for nucleation and growth during solidification, positively affecting quality of castings.

DOI: 10.1007/s11663-016-0807-6

I. INTRODUCTION

CASTING is the manufacturing process in which a molten metal is injected or poured into a die/mold cavity to create a product being either a raw feedstock for further processing or a final component with a near-net or net-shape configuration. Conventional casting offers a limited part quality at a relatively low cost, in contrast to solid-state forming routes, which provide generally better properties but at substantially higher price.[1] The present techniques offering high-quality parts are associated with complex multistep operations exploring the wrought path with additional hot and cold forming, machining, and other shaping processes after casting. As an intermediate measure, there are efforts aimed at reducing the cost of solid state processing and, independently, at improving quality of casting.[2] It is believed, however, that the ultimate solution may only be achieved through development of a novel technology, which will combine the best features of both processes by offering the highest properties typical for wrought products at the low cost and simplicity of casting (Figure 1).

The progress made in the last few decades by the casting industry is associated mainly with the development of new hardware and auxiliaries. This applies, in particular, to high-pressure die casting (HPDC), invented in 1838 for the purpose of producing movable type for the printing industry and since 1894 has been applied for casting of engineering components, being well suited for mass-scale production of bulk metallic parts.[3] At present, HPDC is the major technology of manufacturing parts for the automotive industry. The new machinery, control electronics, tooling and vacuum, robotics and postcasting treatment automation improved the manufacturing outcome and productivity. So far, the hardware improvement is not matched by understanding and exploring opportunities created by molten alloys. There is, therefore, a renewed interest in the processing side of HPDC and other casting techniques especially in controlling the nature of molten metal supplied to the die/mold. At the center of an effort aimed at casting improvement and a quest for a novel technology of large-scale production is so-called liquid metal engineering (LME).[4]

This review provides the fundamentals and applications of LME covering the laboratory- and commercial-scale processes based on both the liquid and semisolid routes. Particular attention is paid to novel elements of LME developed in recent years that combine the melt physical treatment with manipulating its chemistry and temperature to create conditions for optimum nucleation and growth, leading to an improvement of the solidification outcome. A link with conventional treatments aimed mainly at melt alloying, degassing, and purification is emphasized throughout the article.

II. CONCEPTS OF LIQUID METAL ENGINEERING

The term *liquid metal engineering* involves a variety of physical and/or chemical treatments of molten metals aimed at influencing their solidification. Although a simplified approach may limit the phenomenon to

FRANK CZERWINSKI, Innovative Casting Group Leader and Senior Research Scientist, is with CanmetMATERIALS, Natural Resources Canada, 183 Longwood Road South, Hamilton, ON L8P 0A1, Canada. Contact e-mail: Frank.Czerwinski@Canada.ca
Manuscript submitted July 13, 2016.
Article published online October 17, 2016.

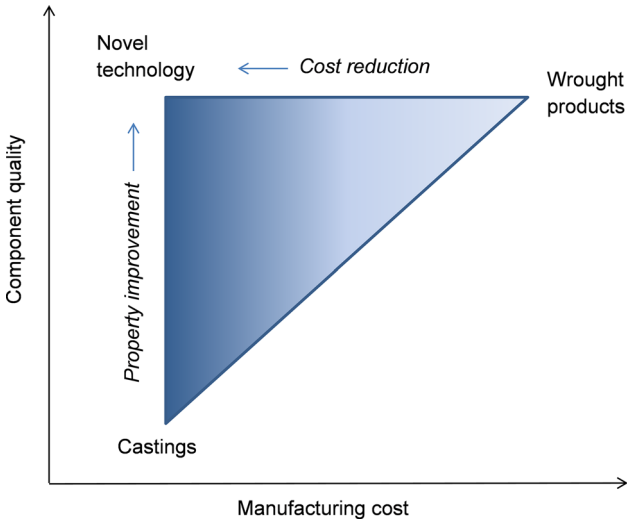

Fig. 1—Schematics showing cost–quality relationships for components manufactured through casting and through solid state forming path. An anticipated location of the novel, single-step manufacturing of net shape components is indicated. Reproduced from Ref. [4] with permission of ASM International.

single-phase molten alloys above the liquidus line, in general, however, it also covers manipulating liquid alloys coexisting with a solid phase, as is the case at temperatures in the liquidus–solidus range.[2]

A traditional approach to liquid metal treatment was limited to alloying to optimize the chemical composition and refining to remove detrimental impurities. Nevertheless, molten alloys are dynamic systems of high complexity and controlling their structural state represents an opportunity of modifying properties of the product formed after solidification.[5] At present, there are varieties of techniques to implement LME and in addition to refining through degassing and filtering, there are also implemented various stirring/shearing/agitations methods based on mechanical, ultrasound, and electromagnetic principles.[6] For example, ultrahigh shear mixing/de-agglomeration solutions, used by food or chemical industries, are also tested with metals. Combining molten alloys with specific temperatures and chemistries is recently explored.[7] This includes chemical modifications for grain refinement with or without melt agitation. The latter may be used to explore internal constituents of melt, *e.g.*, oxide phase inherently present there. When during a process of mixing, thixotropic slurries are used instead of liquid alloys, it opens a way for generating unique alloys and metal matrix composites. In fact, this method may be effective for mixing metals that normally are immiscible.[8] Although LME generally refers to treatment of liquid or solidifying alloys it should be mentioned that the characteristics of two phase slurries may also be affected by their deformation history while in solid state prior to melting.[9]

The liquid alloy treatment may take place either at the stage of raw material generation with a destination for further processing as is the case during semisolid technologies or directly prior to casting into net shape components. Even though at the stage of raw material generation the overall objective may be limited to the alloy microstructure, during forming net-shape components, it must cover both the alloy microstructure and the component integrity. It is worth noting that the opposite approach of manipulating liquid to maximize porosity to create foamed materials is of engineering interest as well.[10] In principle, LME is applicable to all alloys although the present activities are focused on aluminum and magnesium due to their lower melting temperature and therefore less challenging design of the processing hardware.

To avoid confusion, it should be pointed out that the same term of "liquid metal engineering" has been used for decades by the US Atomic Energy Commission for development and non-nuclear testing of liquid metal reactor components, thus, covering entirely different processes and materials.[11] The Liquid Metal Engineering Center and the Liquid Metal Information Center, established in 1966, supported the US Government's Liquid Metal Fast Breeder Reactor (LMFBR) program. Also, outside the United States, the term is used by the nuclear industry with focus on liquid metals in fusion and other energy systems (liquid metal cooled nuclear reactor) with a devoted cyclic International Conference on Liquid Metal Engineering and Technology.[12] The 3rd conference of this cycle, organized by The United Kingdom Atomic Energy Authority in Oxford (UK) in April 1984, placed emphasis on the use of sodium in LMFBRs.[13] Some confusion may also be created by the term *liquid metals* while referring to amorphous alloys, the unique materials that are distinguished by their ability to retain a random structure when they solidify, in contrast to the crystalline atomic structure that forms in ordinary metals and alloys. The same term is incorporated into the company name producing amorphous alloys—Liquidmetal Technologies, Inc.[14]

III. NUCLEATION AND GROWTH DURING SOLIDIFICATION

Solidification is one of the most fundamental nonequilibrium phenomena universal to a variety of materials. The modern science of solidification began in the 1940s with an application of heat flow to predict casting defects[15] and culminated in 1964 with a publication *Principles of Solidification* by Bruce Chalmers.[16]

When a liquid metal is subjected to cooling, it solidifies. Alternatively, solidification may occur as a result of pressure change. After nucleation, solidification is continued by the movement of the solid–liquid interface and atoms are transformed from the disordered liquid state to the more ordered solid state, which is fundamental to metals processing. This phenomenon is not only paramount for castings but also for welding, powder manufacturing by atomization, or wrought components using cast ingots as a raw material. It is also essential for generation of amorphous materials. Although in the past few decades there has been a spike in the amount of research devoted to crystal nucleation, our understanding of crystal nucleation is far from being

complete. The basic elements of nucleation and growth theory during solidification along with its present interpretations, helping to understand the effect of LME on structural refinement of castings, are provided in this section.

A. *Nucleation: Homogeneous, Heterogeneous and Enhanced Heterogeneous*

According to classical theory, the nucleation of a new phase is a stochastic process, involving fluctuations of nuclei to overcome an energy barrier. The clusters of crystalline atoms, seen as a homogeneous crystalline phase clearly separated from liquid by a distinct interface, are considered as macroscopic objects.[17,18]

The total free energy of formation for a spherical crystalline nucleus of radius R is expressed by the sum of a volume term and surface term, respectively:[19]

$$\Delta G^*_{\text{hom}} = \frac{4}{3}\pi R^3 n_s \Delta\mu + 4\pi R^2 \gamma \qquad [1]$$

where n_s is the number density of particles in the solid, $\Delta\mu$ is the difference between the liquid and solid chemical potentials, and γ is the liquid–solid interfacial tension. This ΔG^* goes through a maximum at the critical radius $R_c = 2\gamma/(n_s\Delta\mu)$ (critical nucleus size) and the height of the free-energy barrier is given by:

$$\Delta G^*_{\text{hom}} = \frac{16\pi\gamma^3}{3(n_s\Delta\mu)^2} \qquad [2]$$

Then, the crystal nucleation frequency I per unit volume is obtained as:

$$I = \frac{k}{\tau_t}\exp\left[-\Delta G^*_{\text{hom}}/Tk_B\right] \qquad [3]$$

where k is a constant, k_B is Boltzmann's constant, and T is temperature. According to Eq. [3], the nucleation frequency is controlled by the kinetic factor τ_t, which is the characteristic time of material transport controlling crystallization.

It is a common assumption that an undercooled liquid is in a "homogeneous disordered state" before crystallization. Nevertheless, this statement was questioned recently, offering a novel view of the nature of an undercooled liquid state and the mechanism of crystal nucleation. For example, when researching colloidal liquids, it was proposed that contrary to this common belief, an undercooled state is actually not homogeneous but has transient medium-range structural order.[19] According to this assumption, nucleation preferentially takes place in regions of high structural order *via* wetting effects, which significantly reduce the crystal–liquid interfacial energy and thus promote crystal nucleation. It is argued that this evidence helps solving a long-standing dilemma of a large discrepancy between the rigorous numerical estimation of the nucleation rate on the basis of the classical nucleation theory and the experimentally observed ones.

In practice, the energy barrier to homogeneous nucleation ΔG^*_{hom} can be substantially reduced, when nuclei can form at preferential sites, *e.g.* mold wall, impurities, or catalysts:

$$\Delta G^*_{\text{het}} = S(\theta)\Delta G^*_{\text{hom}} \qquad [4]$$

where $S(\theta)$ is a contact-angle-dependent function and for small contact angles $S(\theta)$ is very small ($\approx 10^{-4}$). A relation between energy barriers for homogeneous and heterogeneous nucleation is shown schematically in Figure 2. As shown in Figure 2(a), for a given energy barrier ΔG, heterogeneous nucleation requires lower undercooling. Figure 2(b) shows a free energy difference as a function of nucleus size. In the case of spinodal decomposition, the supercooled liquid is unstable with respect to the crystalline phase, and the transformation to the crystal proceeds in a barrierless fashion.[18] To take advantage of heterogeneous nucleation, it is important to understand which materials can either promote or inhibit nucleation events.

Over decades, substantial progress has been made in understanding the nucleation of solids in melts at very high undercooling. This is in contrast to nucleation at very low undercooling. According to recent research, for very small undercooling, the process is deterministic, not stochastic.[20] Furthermore, nucleation takes place exclusively on heterogeneities and proceeds as athermal nucleation where the number of nucleation events depends on the undercooling but not on time nor on the mechanism (adsorption, wetting or nucleation) of the initial formation of a thin solid layer on the nucleant area.

The heterogeneous nucleation can be further enhanced by providing substrates for easy nucleation described as nucleation potency. The latter term is defined as the crystallographic lattice mismatching between materials of the substrate and nuclei. The epitaxial nucleation model, proposed recently,[21] assumes that heterogeneous formation of the solid phase on a potent (small lattice misfit) substrate occurs by epitaxial growth of the pseudomorphic solid phase on the substrate surface under critical undercooling (Figure 3). The growth of solid phase progresses by creating misfit dislocations at the interface between the pseudomorphic phase and the potent substrate to transform the pseudomorphic phase into a solid phase followed by coherency change from initially coherent to semicoherent. The critical undercooling ΔT_c during epitaxial nucleation was determined as:[21]

$$\Delta T_c = \frac{\gamma_{LS} + \gamma_{SN} + \gamma_{LN}}{\Delta S_v h_c} \qquad [5]$$

where γ_{LS}, γ_{SN} are interfacial energies after the epitaxial nucleation: γ_{LS} between liquid phase L and solid phase S and γ_{SN} between solid phase S and nucleation substrate N. The interfacial energy γ_{LN} is between liquid phase L and nucleation substrate N before epitaxial nucleation. In this equation, ΔS_v is the entropy of fusion per unit volume and h_c is critical thickness of the pseudomorphic layer. Equation [5] allows calculating the critical undercooling ΔT_c under which the pseudomorphic layer is able to grow to critical thickness h_c. This mechanism is explored for improvement of alloy properties through grain refinement.

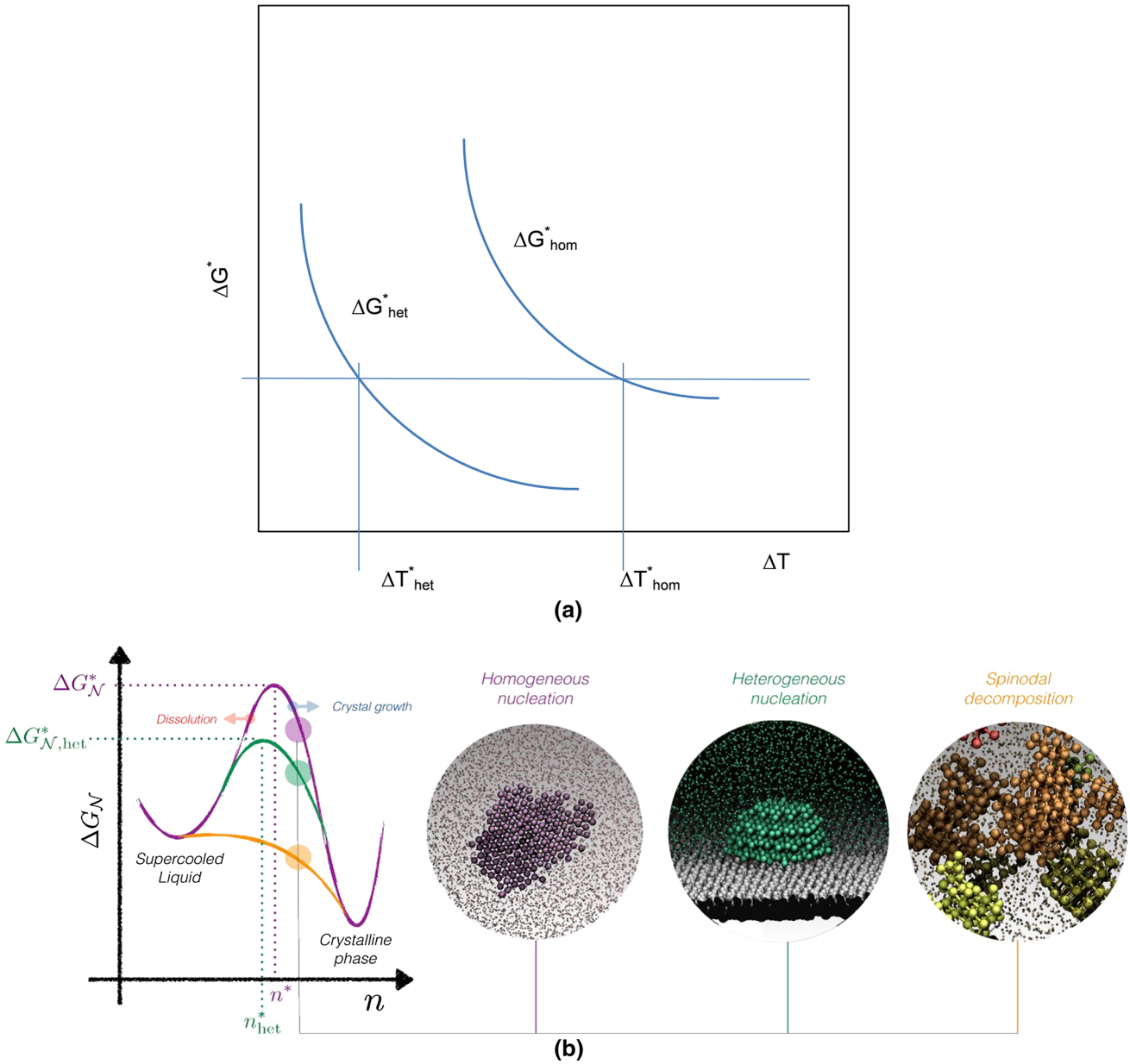

Fig. 2—Energy barriers of solidification nucleation: (*a*) schematic of energy barriers for homogeneous ΔG^*_{hom} and heterogeneous ΔG^*_{het} nucleation under certain undercooling ΔT, showing an advantage of the latter. As seen in the plot for a given energy barrier ΔG^*, the heterogeneous nucleation requires lower undercooling. (*b*) Schematic showing free energy difference ΔG^*_{N} as a function of the crystalline nucleus size n for homogeneous ΔG^*_{N}, heterogeneous $\Delta G^*_{\text{N,het}}$ nucleation and spinodal decomposition along with views of crystalline cluster nucleating within the undercooled liquid in each case. Fig. (b) reproduced from Ref. [18] with permission of MDPI, Basel, Switzerland.

B. *Growth*

After a nucleus is formed, solidification enters the stage of growth. If the enthalpy of the solid is less than that of the liquid, the process may generate heat. Similarly, solute may partition into the liquid if its solubility in the solid is less than that in the liquid. The accumulation of solute and heat ahead of the interface can lead to circumstances in which the liquid in front of the solidification front is undercooled. The interface thus becomes unstable, and in appropriate circumstances, solidification becomes dendritic. When regular cells grow at a relatively low rate they grow perpendicular to the liquid–solid interface regardless of crystal orientation.

The microstructure formation in metal castings may be predicted from a model of solute diffusion.[22] At higher growth rates, the crystallographic factor takes control of the growth direction, which deviates toward preferred crystallographic orientation. A dendrite tends to branch because the interface instability applies at all points along its growth front. As a result of branching, the growth front has a tree-like character, which is the origin of the term *dendrite*. The essential role of convection and fluid

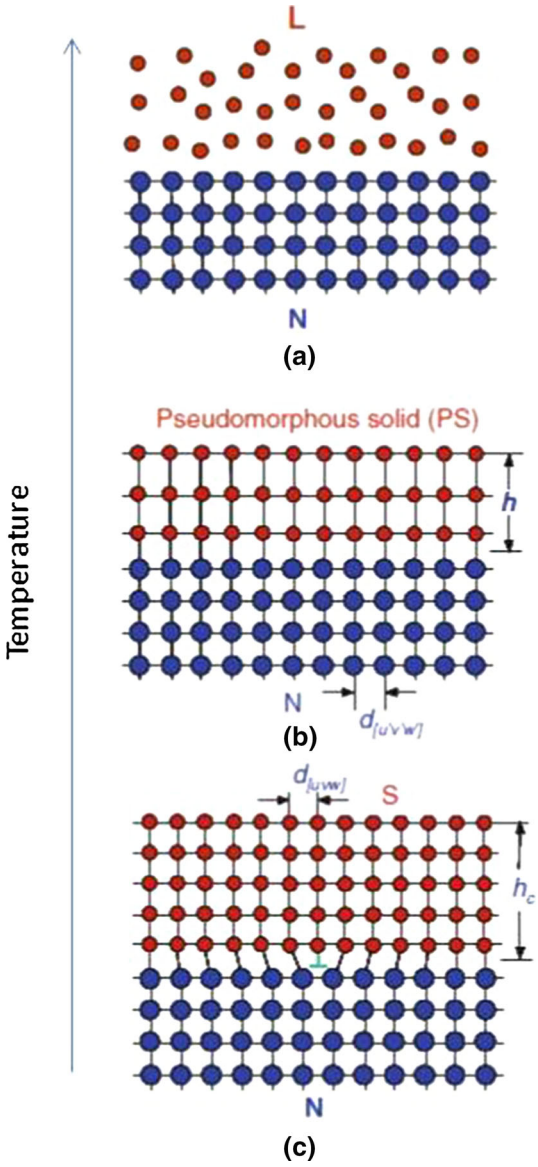

Fig. 3—Epitaxial model for heterogeneous nucleation of a solid phase S on the potent substrate N from liquid phase L: (*a*) initial state before formation of the pseudomorphic layer; (*b*) formation of the pseudomorphic layer with coherent interface with the substrate; and (*c*) nucleation completed by formation of misfit dislocations and interface conversion to the semicoherent one. Adapted from Ref. [21] with permission of Springer.

flow during solidification and crystal growth is well established.[23]

When considering LME at temperatures in the solidus–liquidus range, the question arises as to whether the external force applied during solidification can cause mechanical deformation of dendrites. According to common belief, fluid flow during solidification does not exert mechanical effect on growing dendrites. As stated in Reference 24, there is no evidence reported in the literature that dendritic arms were mechanically bent as a result of the external force. Numerical simulations concluded that, under most conditions possible during solidification, the likelihood of mechanical damage of dendrites is remote.[25] Nevertheless, the twin condition required for dendrites to deform; *i.e.,* very thin dendrite accompanied by high flow velocity of melt can exist in undercooled melts as verified for Cu-O and Cu-3 wt pct Sn systems.

Modern X-ray techniques allow *in situ* observations of nucleation and growth of individual grains during solidification within the bulk of liquid metals, offering the opportunity to validate the theoretical models.[26] For Al-Ti-B alloys, the metastable $TiAl_3$ phase was identified as being responsible for enhanced nucleation. After the formation of aluminum grains, the $TiAl_3$ phase subsequently dissolved at the expense of the more stable solid aluminum-titanium alloy. An example of real-time observations of nucleation and growth for selected chemistries of the Al-Ti-B system is shown in Figure 4. The growth curves of individual aluminum grains with and without added TiB_2 particles show a close resemblance to the behavior of the solid fraction. For diffusion-controlled growth of noninteracting grains, the grain radius $R(t)$ as a function of time t is given by:[25]

$$R(t) = \lambda_s \sqrt{D_s(t - t_s)} \qquad [6]$$

where λ_s is a parameter determined from the titanium solubility in the liquid and the solid phases, D_s is the diffusion constant of solute titanium in the liquid, and t_s is the moment of nucleation of the grain.

For decades, there has been a discussion to determine which of two stages, nucleation or growth, exerts a larger effect on the casting structure. There is a merit in the recent tendency toward emphasizing the paramount role of nucleation. Nevertheless, to take full advantage of solidification, both stages, nucleation and growth, should be understood and explored.

IV. IMPROVING CLEANLINESS OF MOLTEN METALS

Molten metals, especially those with high reactivity like aluminum, have a tendency to absorb hydrogen gas from the atmosphere, and the ability to readily oxidize. Moreover, impurities may form due to reactions with refractories and crucible walls and due to alloying additions to the melt. A control and removal of gas and solid impurities from molten metals is of key importance to produce quality castings. There is a tight link between conventional melt treatments and new concepts of LME. For any manipulation aimed at modifying solidification microstructure, melt cleanliness is essential. In addition, during majority of novel LME treatments, melt degassing and purification is superimposed on other processes of melt agitation.

A. *Degassing*

Molten alloys are susceptible to entrapped and dissolved gasses, which after solidification have a detrimental effect on the mechanical properties of castings. As examples of gas sources, fossil fuel decomposition and chemical flux material or alloy additives are frequently given. Also, water from moist air or wet tools

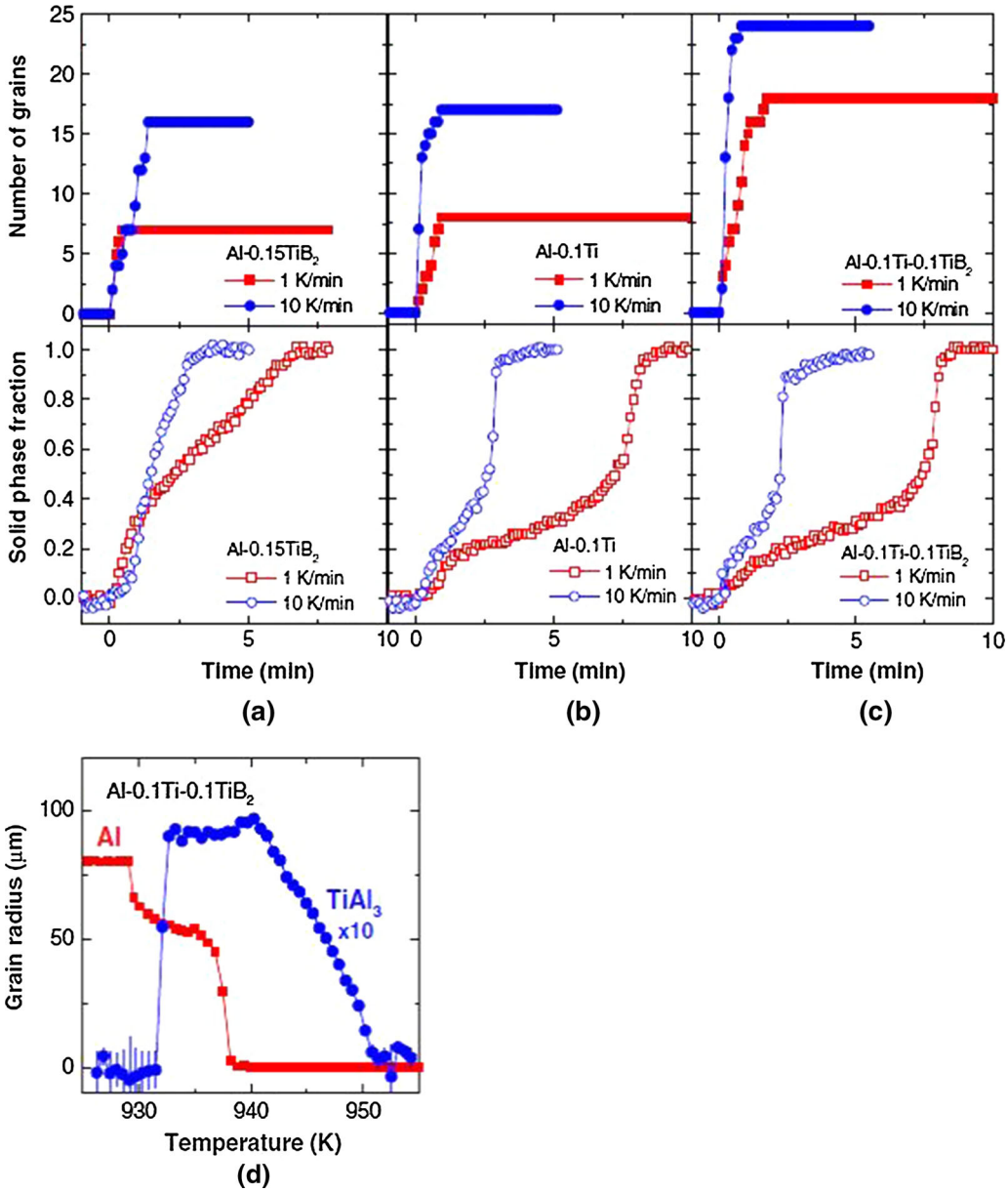

Fig. 4—Real-time observations of solidification of Al-Ti-B alloys using X-ray methodology: (*a*) through (*c*) grain nucleation and solid fraction as a function of time for cooling rates of 1 K/min and 10 K/min (1 °C/min and 10 °C/min); (*d*) grain growth of Al and metastable $TiAl_3$ as a function of temperature. Reproduced from Ref. [26] with permission of Elsevier.

decomposes to release hydrogen in the melt. In the case of reactive metals such as aluminum, the typical phenomenon is adsorption and dissolution of hydrogen in its liquid state. Then, during solidification, dissolved hydrogen transforms into porosity within aluminum alloys, which is detrimental to the mechanical properties of castings and forgings. Thus, in addition to preventing the entering of hydrogen into the melt from outside, measurements of its content and subsequent removal are standard procedures prior to casting.

Vacuum degassing is used primarily in the steel industry.[27] The present degassing techniques of aluminum include rotary impeller degassing and the flux injection process in addition to traditional purge gas insertion methods, which is seen as less effective.[28] An example of a commercial concept is shown in Figure 5. The overall mechanism is that inert gas collects the soluble hydrogen atoms, leading to hydrogen molecule formation inside the lower pressure of the collector gas bubble. As a purge (collector) gas, the most commonly used is nitrogen. Argon, being heavier, provides better cover around the melt and produces less metal-rich dross. Active halogens are used as well to improve the efficiency of degassing with an inert gas.

In a technique patented in the 1960s, a flushing cap device is used in conjunction with a lance injection tube for more efficient removal of gasses.[29] As a flushing medium, nitrogen or other similar gases are used. The removal of dissolved gases occurs by diffusion from the metal into the bubbles of the inert gas. As long as the

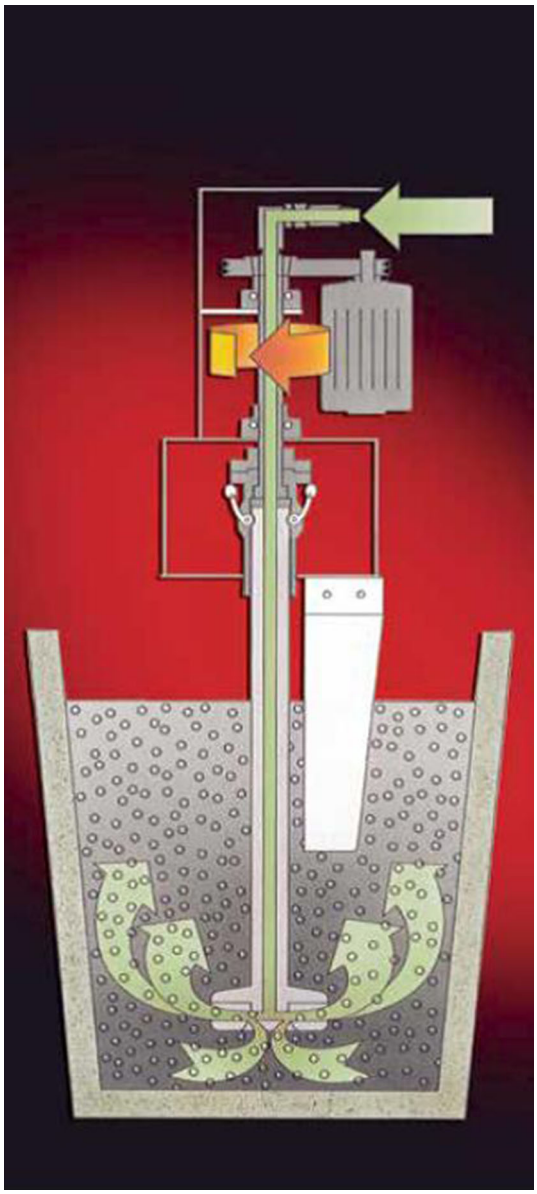

Fig. 5—Design of foundry degassing unit (FDU) for an improvement of quality of nonferrous castings based on the impeller principle with rotor, which mixes an inert gas, usually nitrogen or argon, with the melt. The gas bubbles are distributed widely through the melt while maintaining a smooth melt surface resulting in short treatment times, effective degassing, and melt cleaning. Courtesy of Foseco, http://www.foseco.com.

hydrogen diffuses freely from the metal, flushing for a certain period of time lowers the concentration of hydrogen in the melt. During purging of the melt with gas, the surrounding atmosphere affects the rate of hydrogen removal since the molten bath tends to reabsorb hydrogen by reacting with atmospheric moisture and absorbing hydrogen from combustion products. Therefore, an oxygen-free atmosphere overlying the molten metal, such as dry nitrogen, is provided. The rotary impeller degassing, introduced in the 1980s, relies on feeding the purge gas through a rotating shaft, impeller, or rotor. The finer bubbles, formed in this technique, reside for a longer time inside the melt, collecting more hydrogen atoms. In the 1980s, Pechiney developed the IRMA™ (Injecteur Rotatif en four de MAintien) process based on introduction of gas bubbles in the melt through the use of rotary impellers accessing the furnace through the roof.[30]

B. *Combining Gas With Fluxes*

To improve the quality of the aluminum melt, in addition to nonmetallic inclusions and hydrogen, dissolved alkalis like sodium and calcium need to be removed. To improve the effectiveness, rotary degassing is combined with a floatation treatment using a variety of fluxes.[28,31] The flux is delivered by a purge gas of nitrogen or argon. The flux should have a granular morphology that flows and should melt only after entering the molten alloy.[32] Since the process in addition to finely dispersed argon uses chlorine, hexachloroethane, C_2Cl_6, and other products, it requires environmental considerations. For example, covering fluxes that form a molten layer to help protect the melt from oxidation and hydrogen pickup. Directly before pouring, so-called *drossing-off fluxes* are added to react exothermically to allow recovery of some aluminum from dross and agglomerating the oxides for easy removal. The cleaning fluxes remove nonmetallic inclusions by agglomerating them together with dross. Fluxes are also added to remove the oxide buildup from furnace walls.

To remove impurities from the melt on a casting line, in-line refining (degassing) equipment is typically installed between the holding furnace and the casting equipment.[33] The main element of the Rotary Flux Injector™ by STAS[34] is the spinning nozzle, through which a carrier gas (nitrogen) delivers the fluxing agent (solid salts) underneath the metal surface. The liquefied fluxing agent is dispersed through the combined actions of the disperser and the injection of the carrier gas. It is claimed that the design significantly improves the efficiency of the fluxing process. An effective solution was also achieved by Melt Treatment System 1500,[35] a rotary degassing vortex treatment along with a specially developed flux that reduced the amount of dross created and produced dross with a lower metal content, therefore, minimizing the metal loss. The high cleanliness of the melt resulted in better fluidity, die filling, and extended feeding distances. Also the volume fraction, size, and location of porosity were positively affected.

C. *Ultrasonic Degassing*

The possibility of using ultrasonic technology for metal degassing was first suggested in the 1930s. Yet, successful industrial application of ultrasonic degassing light alloy melts was only accomplished in the 1960s when essential relationships were established between the hydrogen removal and cavitation development.[36] The primary physical phenomenon associated with ultrasound that is relevant to treatment of molten metals is acoustic cavitation. It relies on the formation, growth, and implosive collapse of bubbles in a liquid that creates extreme conditions inside the collapsing

bubble and serves as the origin of most sono-chemical processes.[37]

After a liquid metal is subjected to ultrasonic vibrations, the alternating pressure above the cavitation threshold generates bubbles in the liquid, which first grow than collapse. When cavitation develops, mass transfer intensifies causing the diffusion of dissolved hydrogen toward the bubbles and then along with them to the melt surface.[38] The versatility of ultrasonic applications includes, in addition to degassing, different effects on liquid metal such as grain refinement and segregation control.[39]

One experimental ultrasonic degassing method uses high-intensity ultrasonic vibrations to generate oscillating pressures in a liquid metal.[40] A treatment of aluminum alloys in air, under vacuum and in a combination with an argon purge, were able to remove gas within a few minutes of ultrasonic vibration, much faster than traditional degassing methods. It is of interest that the ultrasonic degassing efficiency was increased by small volumes of purge gases. Also, the amount of dross was reduced by more than 50 pct. In fact, recent concepts of the ultrasonic device comprise an ultrasonic transducer with a probe and a gas outlet at or near the tip of the probe.[41] Another improvement was achieved by combining ultrasonic degassing with mechanical stirring.[42] For fixed ultrasonic parameters, the degassing efficiency and casting porosity depended on the melt temperature and on the rotation speed of the mechanical stirrer.

In addition to testing new hardware designs, experiments were performed for specific commercial alloys. For the AlSi9Cu3 aluminum alloy (all alloy compositions are given in wt pct), the degassing rate was four times higher as compared to the gas purging method.[43] When using hardware based on the novel multifrequency multimode modulated technology, it was found that ultrasonic degassing is effective in reducing porosity as well as in improving the final density of AlSi9Cu3 castings.[44] As stated, the effectiveness of ultrasound in degassing and in removing impurities from molten metals can be increased by an addition of a purging gas into the molten metal bath in close proximity to the ultrasonic device.[45] Research with melt quantities of up to 150 kg confirmed earlier laboratory tests that a moving ultrasound probe could achieve results similar to those of the argon process but with an advantage of not relying on expensive and fragile graphite rods and expensive gas that cannot be captured and recycled.[46] Treating molten metal with ultrasound is cleaner and more efficient than using argon rotary degassing to produce high-quality castings. Nevertheless, despite promising laboratory tests, the commercial application of ultrasonic degassing is still very limited.

D. *Removal of Inclusions*

There are several methods to remove inclusions from molten metals to prevent slag, dross, or pieces of refractory from the melting crucible entering the casting, including:[47]

(i) Filtration where molten metal and inclusions are separated by porous media
(ii) Sedimentation where particles agglomerate on the bottom of the molten metal
(iii) Flotation where inclusions congregate on the surface of the molten metal
(iv) Centrifugal separation where inclusions are removed by rotating filters due to the density difference

These techniques replace an older approach of removing inclusions through whirl gates and extensive runner systems.

Several established filter technologies are available including strainer cores, woven cloth or mesh, and ceramic tile filters, with the latter being considered as the most effective.[48] The most popular solutions include pressed cellular, extruded cellular, and foam filters. The pressed cellular filters are generally characterized by their round cells when extruded ones have square cells and foam filters have a random dodecahedron-type structure. Selection of an appropriate filter depends on melt chemistry and pouring temperature, amount and type of slag or inclusions, and expected performance factors such as the throughput rate.[49] For example, the standard ceramic cellular or reticulated foam filters are not readily adaptable to highly automated die casting and permanent mold casting operations. Ceramic honeycomb filters[50] featuring large surface area, high mechanical strength, and good thermal shock resistance are mainly used in the foundry environment. In metal casting, honeycomb ceramic filters remove impurities and reduce casting porosity leading to improved casting quality (Figure 6(a)).

Ceramic foam filters (CFFs), introduced in late 1970s,[51] have wide application in molten metal filtration (Figure 6(b)). Reticulated CFFs are widely used in the foundry because of their high permeability and excellent filtration efficiency.[52] Ceramic foams have a three-dimensional reticulated structure and excellent properties including high-temperature resistance, chemical corrosion resistance, low bulk density (0.25-0.65) g/cm^3, and large surface area as a result of high porosity (60-90 pct). CFFs operate in a mode of deep bed filtration with inclusions smaller than the pore openings being retained within the filter. This type of filter is meant for single use so they are replaced after every cast.

Ceramic foam filters, specifically their design[53] and manufacturing techniques,[54] are subjects of extensive research. Also filtration mechanisms are studied with details of the inclusion removal in aluminum alloys and the use of alternative filter materials. The filtration mechanism comprises two parts: (1) transport of inclusions to the filter wall and (2) entrapment of inclusions by the filter wall. Of particular importance are phenomena of collision by interception and wetting (surface tension) between inclusion and aluminum and between filter and aluminum. For effectiveness of filtration, particles to be removed should directly contact or at least reach the vicinity of the filter wall. To accomplish this, the metal carrying the inclusions must wet the filter material.

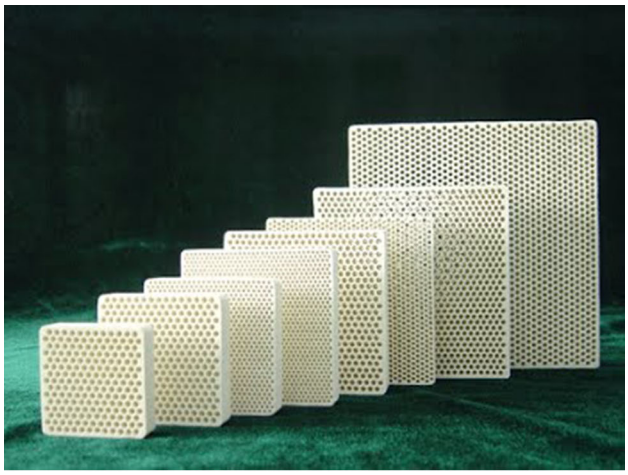

(a)

(b)

Fig. 6—Ceramic filters used for molten metal filtration: (*a*) honeycomb filter[50] and (*b*) foam filter.[51] Courtesy of Induceramic Inc.

Foam filters are produced from several ceramic materials, the composition of which depends on the type of metal subjected to filtration.[55] In addition to wetting melt, filters should be characterized by high thermal shock resistance, resistance to the corrosive effect of metal melts, mechanical strength at high temperatures, and effectiveness of the filtration process. It is of interest that in aluminum filtration, alumina is the most common filter material, even though alumina is not wetted by aluminum.[56] Alumina filters show the best combination of high thermal shock resistance and filtering efficiency.[57]

For cast steel, where temperature reaches 1923 K (1650 °C), ZrO_2-based filters are currently applied.[58] Trials of cast steel filtration using two types of newly developed foam filters in which carbon was the phase binding ceramic particles have been conducted. In one filter, the source of carbon was flake graphite and coal-tar pitch, whereas in the other one, graphite was replaced by a cheaper carbon precursor.[59]

Despite widespread use of metal filtration, ceramic filters have several drawbacks that limit their applicability. Although filter preheating is applied, they tend to be clogged by freezing particles on the first contact with the molten metal. To prevent clogging, metal is overheated by at least 100 K (100 °C), negatively affecting melt stability and increasing consumption of energy. To eliminate the need of overheating, carbon coatings have been applied to the surface of ceramic filters to reduce the thermal mass of the part that comes into direct contact with the molten metal.[60] As a further improvement, the filter comprising a major ceramic phase and a minor carbon phase bonded by a phosphate compound was proposed.[61]

V. PHYSICAL TREATMENT OF MOLTEN METALS

External forces (stress) applied to a molten alloy to initiate flow within it, an effect generally referred to as *agitation*, result in macroscopic and microscopic mass transport that assists a distribution of heat and chemical constituents, therefore, affecting solidification. Although there are many techniques of physical treatment of molten alloys, three major categories including stirring, vibration, and impact are most often distinguished.[62] The specific terminology is not consistent throughout the literature, and to draw a conclusion, the device used to interact with the melt should first be assessed. Advantages of agitation of a molten metal were noticed as early as in 1870 where experiments on steel showed that the shaken melt developed after solidification a much finer grain structure.[63] This review is not focused on activities during primary steps of alloy generation but on treatments explored during molten metal processing prior to casting final components.

A. *Mechanical Stirring*

Mechanical stirring is accomplished by augers, impellers, or various shape agitators attached to rotating shafts. An advantage of mechanical stirring is that its impact on the melt can easily be quantified through measurements of torque, geometry, and rotational speed of the mixer. By analogy with solids, one type of deformation of molten metal under stress is shear. To create flow in a molten metal, a stress must be applied. Under an applied force F to the area A, one type of deformation is shear τ expressed as:

$$\tau = \frac{F}{A} \qquad [7]$$

The shear rate $\dot{\gamma}(s^{-1})$ in a system under a force describes the rate of change of velocity v with distance h and is defined as:

$$\dot{\gamma} = \frac{v}{h} \qquad [8]$$

A resistance of a liquid to deform is referred to as viscosity. The fundamental relationship between a force and deformation in liquids is the subject of rheology.

The concept used to exert a shear on liquids originates from the late 1800s and relies on concentric cylinders with a uniform gap around the inner cylinder. The cylinders are rotated either independently of each other or together in the same or opposite directions (Figure 7). The rotation generates shear forces within the liquid held in the gap between cylinders, which is measured as torque. When the inner cylinder rotates and outer cylinder is fixed (with no torsion wire), the design is called the Searle type. When the outer cylinder rotates and inner cylinder is suspended by torsion wire, the design is called the Couette type. A modification was introduced in the 1930s[64] with a conical slope at the end of the inner cylinder to ensure the shear rate is uniform throughout the fluid volume, even in the region under the inner cylinder. The same ideas were later adopted for molten metals. For both methods, Searle and Couette, the shear stress is calculated for the inner cylinder:[65]

$$\tau = \frac{M}{2\pi l_b R_b^2} \quad [9]$$

where M is the torque of the inner cylinder, R_b is the radius of the inner cylinder (bob), and l_b is the immersed depth of the inner cylinder. The experiments with Couette-type viscometers in the early 1970s led to the original observation that stirring of molten alloy during solidification leads to thixotropic morphologies instead of to dendritic forms.[66] As explained at that time, melt shearing caused "breaking up dendrites."

A distinction is made between active stirring, where shear is directly induced, and passive stirring, where molten metal is forced to flow through stationary narrow channels.[67] The latter takes place at the injection stage of die casting or injection molding when metal flows at very high velocity through the gating system to fill the mold/die cavity. In case of thin wall casting, high velocities accompany flow of the melt inside the part as well (Figure 8).[68] To magnify the mixing effect by injection screws in plastics molding, static mixers of complex geometry are introduced to the melt flow path.

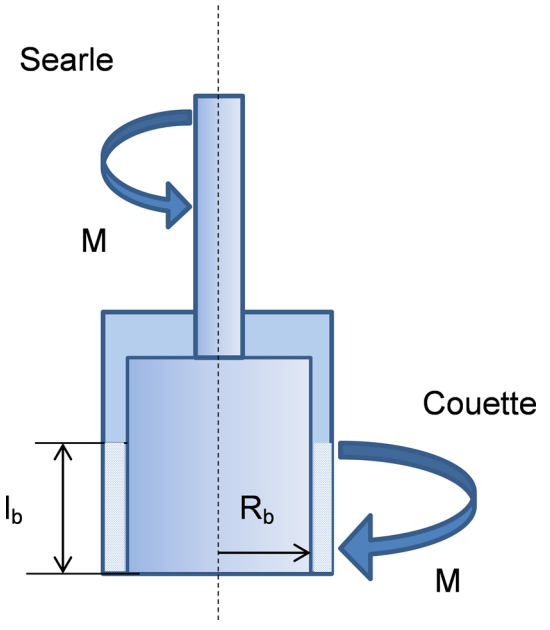

Fig. 7—Schematics of Couette/Searle device to impose shear on molten metals. Differences between Couette and Searle concepts are indicated.

Examples of hardware solutions where mechanical stirring is explored include continuous mechanical stir caster,[69] injection molding machinery with its reciprocating screw action,[2] or shearing cooling rolls. A scaled-down casting concept with two intermeshing screws within the twin barrel (cylinder), fed with a liquid alloy, was explored in a laboratory environment.[70] It should be noted that the twin screw design, based on a rheo-processing principle, is essentially different from the single screw commercial system based on the thixo-processing concept, which is fed with solid coarse metal particulates called chips, pellets, or granules.[2]

In hardware designs, using barrel and reciprocating injection screws, the material is sheared between two surfaces that move in relation to each other, *i.e.*, the barrel inner wall and root of the screw (Figure 9). As the relative speed between screw and barrel increases and the radial distance between them becomes smaller, the shear increases. At any single point along a screw, the shear can be calculated as:[71]

$$S = \frac{DN}{219.1h} \quad [10]$$

where S is the shear rate (reciprocal seconds); D is the screw diameter (mm); N is the screw speed (rpm); and h is the screw channel depth (mm). The literature description of processing mechanisms inside the injection molding barrel, including shearing phenomenon, refers predominantly to plastics. A replacement of high-viscosity plastics with low-viscosity metal leads to essential differences with details described in Chapter 5 of Reference 2.

B. *Mechanical Mold Vibration*

Agitation of a molten alloy may be achieved through mold vibration. An advantage of this method is that no mixers are inserted into the melt, helping to avoid corrosion. For practical reasons, frequencies used are rather low. The effect of mold vibration with a frequency up to 20 Hz on the solidification structure was verified for an Al-Si eutectic alloy and gravity die casting.[72] The mold vibration caused refinement and improved uniformity in distribution of the eutectic silicon. Also, the α-Al dendrites experienced refinement. The alloy developed increased tensile strength and hardness after post-cast heat treatment with the highest values recorded for the frequency of 15 Hz.

A similar range of vibration frequency up to 24 Hz was tested for the AZ91D magnesium alloy.[73] It was concluded that the mold vibration during melt solidification caused grain refinement and improvement of mechanical properties. The optimum frequency of mold vibration was between 12 and 16 Hz. The same vibration frequency range 12-16 Hz was optimal for an

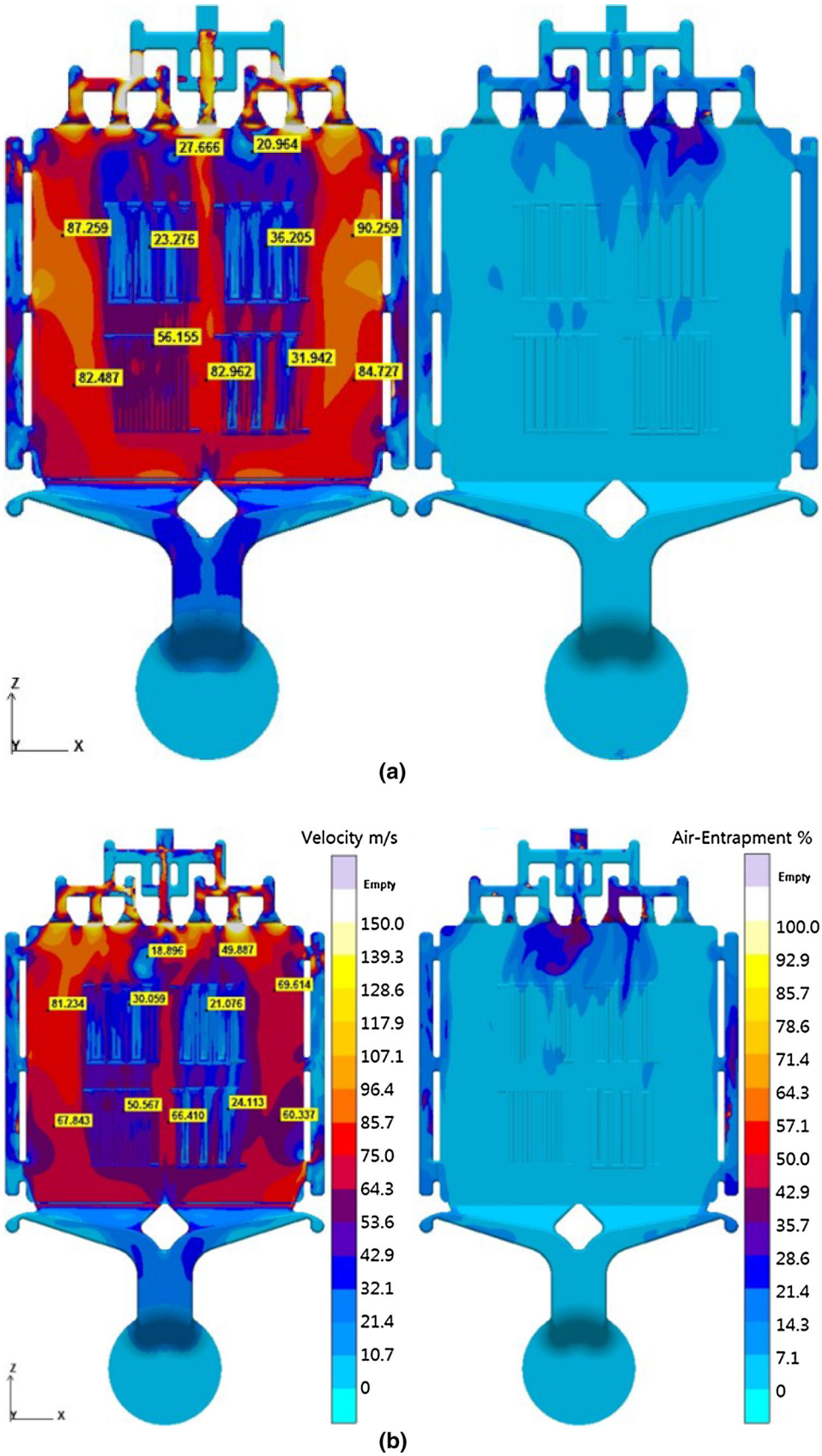

Fig. 8—Velocity distribution of the melt and air content in the die cavity using different plunger speeds in vacuum high-pressure die-casting: (*a*) plunger speed of 3.0 m/s and (*b*) plunger speed of 2.5 m/s. Silafont-36 (AlSi9MgMn) alloy. Reproduced from Ref. [68] with permission of MDPI, Basel, Switzerland.

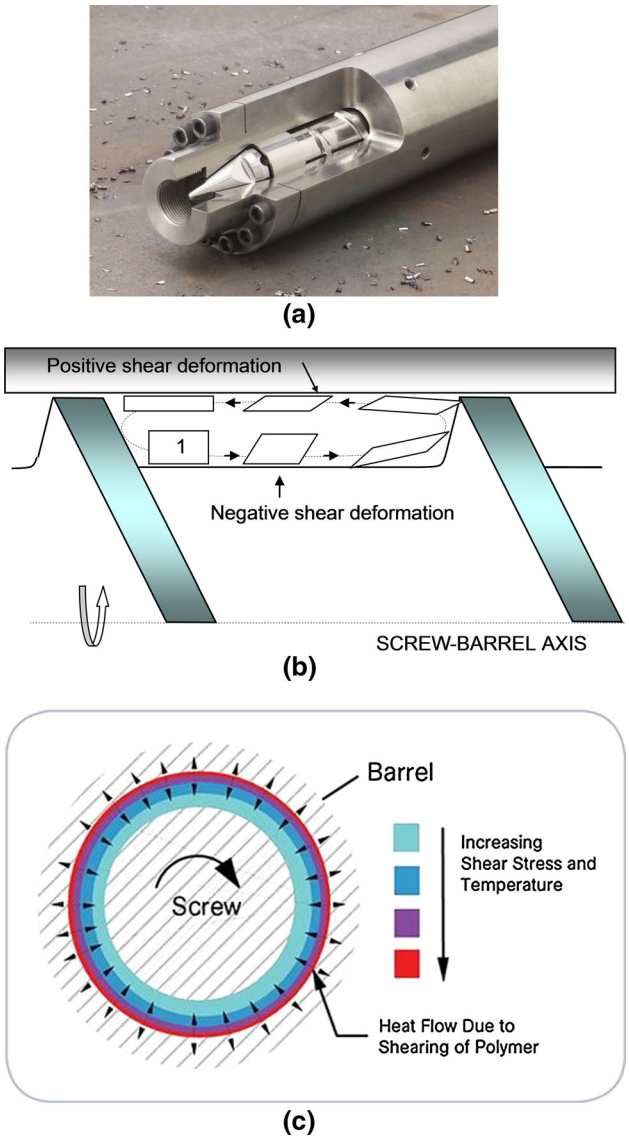

Fig. 9—Mixing and shearing of a material by injection screw/barrel couple: (*a*) a view of injection screw inside the barrel; (*b*) shearing details during screw rotation; and (*c*) shear distribution inside the barrel as determined for polymers. At present there are no proven data for molten metals. Figures: (a) courtesy of CONCOR—Tool and Machine, http://www.concortool.com; (b) reproduced from Ref. [2] with permission of Springer; (c) reproduced from Ref. [175] with permission of Gardner Business Media, Inc.

improvement in thermal conductivity and diffusivity of Al/TiC composites.[74] A higher frequency in the range from 40 to 150 Hz was tested using Al-6 wt pct Cu alloys.[75,76] The vibration was introduced when the melt reached 973 K (700 °C) and continued until complete solidification. An increase in vibration frequency from 40 to 150 Hz was accompanied by a finer grain size and by an increase in alloy hardness. In conclusion, no chemical additives for grain refinement were required.

C. *Concept of Ultrahigh Shear Mixing*

The ultrahigh shear mixers are designed for applications that are beyond the capabilities of a conventional agitator or stirrer. The terminology of "ultrahigh shear mixing" came from nonmetallurgical applications where rotor–stator devices called high-shear mixers were introduced for high-volume de-agglomeration offering many advantages compared to traditional colloid mills, media mills, immersion mills, and high-pressure homogenizers.[77] The concept is widely used across processing industries, including chemical, cosmetic, food, pharmaceutical, adhesives, and plastics for emulsification, homogenization, blending, dissolving, de-agglomeration, particle size reduction, and dispersion of solid particles or gas suspended in liquid. Such devices are operated either in batch or inline arrangements. For example, in-line high shear mixing followed by adsorption was found to be effective for desulfurization of diesel fuel.[78] Typical applications, power draw, and flow characteristics of rotor–stator mixers have been reviewed in References 79 and 80.

In a typical design, a rotor or impeller, together with a stationary component known as a stator, or an array of rotors and stators, is used either in a tank containing the solution to be mixed, or in a pipe through which the solution passes, to create shear. A specific example of design of an ultrahigh shear mixer for other media than molten metals represents a rotor–stator configuration with unique geometries and multistage arrangements of concentric intermeshing teeth. The mixed material moves through channels of the rotor and stator teeth with very close tolerances between adjacent surfaces, thereby experiencing very high shear.[81] A different design explores high-velocity pumping vanes that force the material into semicylindrical grooves where it splits into different streams colliding at a high frequency before leaving the mixer.[82]

In another rotor–stator design, a rotor with a diameter of 85 mm has four blades and the stator has 72 slots on the side with 8 holes on the top.[83,84] According to computer modeling, the maximum stress was located in the rotor–stator gap. The modeling also showed that a minimum speed is required below which the rotor–stator mixer cannot be used. The ultrahigh shear-stator rotor design shown in Figure 10 was recently tested with chemical solutions. As verified by computational fluid dynamics, the residence time distribution in the measurement outlet agreed with the outlet flow.[85] Due to the essential difference between media used by other industries and molten metal, mainly the temperature range and corrosive attack, the hardware design is not universally interchangeable. Nevertheless, a combination of a simple rotor–stator unit is also adaptable for metallurgical processing. This concept is used to generate an intensive melt shearing to disperse effectively the harmful inclusions into fine particles and enhance nucleation during subsequent solidification.[86]

D. *Electromagnetic Stirring*

The essence of electromagnetic stirring is the current J:

$$J = \frac{1}{\mu} \nabla \times B \qquad [11]$$

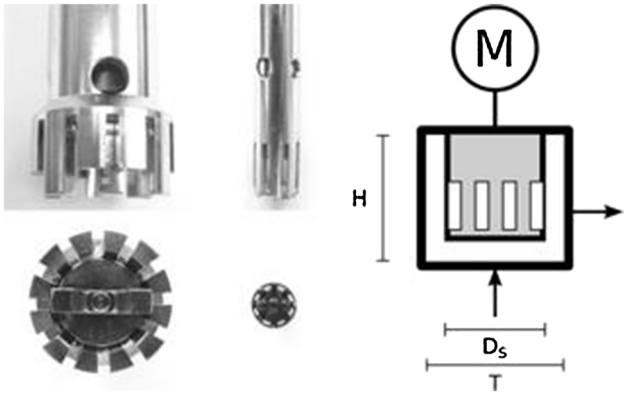

Fig. 10—Design example of ultrahigh shear mixer based on cylindrical stator–rotor: schematic diagram of the reactor (right), 2.5-mL rotor–stator (center), and 9.5-mL rotor–stator (left). 2.5-mL reactor diameter (T) 13 mm, liquid height (H) 22 mm. 9.5-mL reactor diameter (T) 30 mm, liquid height (H) 15 mm. Reproduced from Ref. [85] with permission of John Wiley & Sons.

generated in the liquid metal according to Faraday's law when alternating current circulates through coils placed around the crucible (μ magneto conductivity, B magnetic intensity). The electromagnetic, Lorentz force $F = J \times B$, imposed on molten metal, is expressed as:[87]

$$F = \frac{1}{\mu}(\nabla \times B) \times B = (B \times \nabla)\frac{B}{\mu} - \nabla\frac{B^2}{2\mu} \qquad [12]$$

indicating the whirling force stirring the melt (first component of equation) and radial restriction force (second component). A schematic of power modules (poles) arrangements of an industrial device along with an example of molten metal velocities modeled are shown in Figure 11.[88]

The electromagnetic technologies are used for ferrous and nonferrous metals.[89] The key limitation of this method is its scalability. According to Reference 90, an industrial-size ingot requiring relatively intense steady magnetic-field strength inside an air gap on the order of 300 mm width would require a current intensity of about 40,000 A. To reduce energy requirements, a solution based on an extension of the so-called Helmholtz resonator was proposed.[91] The Helmholtz resonator consists of a bottle almost entirely enclosing a volume of air, with a small opening constituting a coupling between the air in the bottle and the external air of the room. As shown in Figure 12, the resonator consists of a cavity with a liquid metal, where the neck is crowned by a small pulsating electromagnetic pump; this pump plays the role of an exciter for the resonant cavity. An alternating voltage is applied between the two electrodes while the pump is subjected to a stationary magnetic field perpendicular to the variable electric current. In this design, the cavitation threshold depends mainly on the electromagnetic pressure peak, and under well-developed cavitation, a very fine and homogeneous microstructure was obtained.[90]

In another design, exploring the electromagnetic principle, the horizontal stirrer contains three phases and three poles, with each phase located circumferentially so that the

(a)

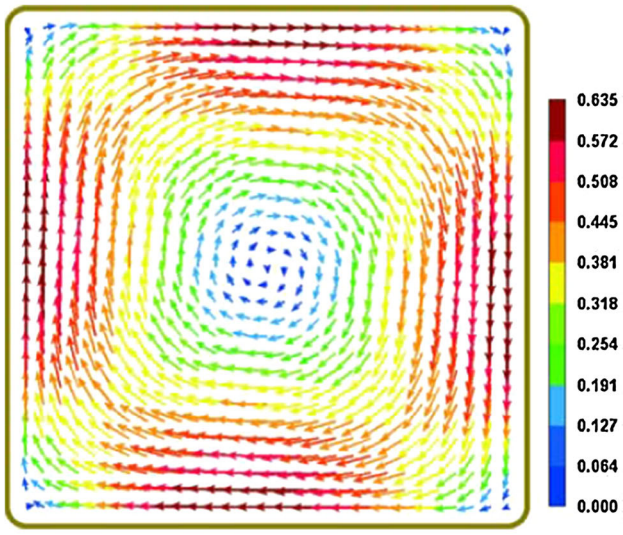

(b)

Fig. 11—Simplified diagram of a unit for modeling magnetohydrodynamic processes in the mold of a continuous section caster (*a*) and velocity field (m/sec) in the cross section of the mold (center of the stator) for I = 150 A and f = 6 Hz (*b*). Reproduced from Ref. [88] with permission of Springer.

current flows through the coils.[92] The electromagnetic force, oriented toward the circumferential direction, causes refinement of the α-Al phase in an A356 aluminum alloy. Another proof of concept was verified through an annular electromagnetic stirring unit. The device was used to assess the effect of cooling rate, stirring power, and stirring time on the solidification behavior of A357 alloy.[93] As expected, increasing the cooling rate and stirring power caused higher grain refinement. The fully refined equiaxed grain structure was obtained within 10 seconds of processing. It is believed that the uniformity of temperature and chemical composition during the initial stage of solidification increased the effective nucleation rate.

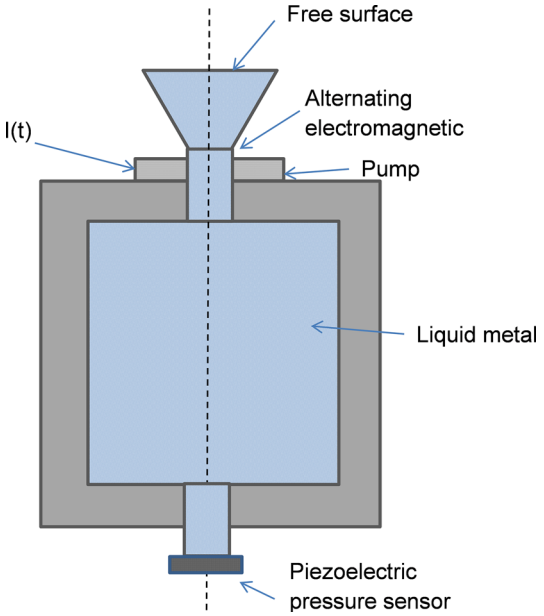

Fig. 12—Magnetohydrodynamic cavity resonator designed to increase effectiveness and reduce the extremely high current intensity required. Adapted from Ref. [90] with permission of Springer.

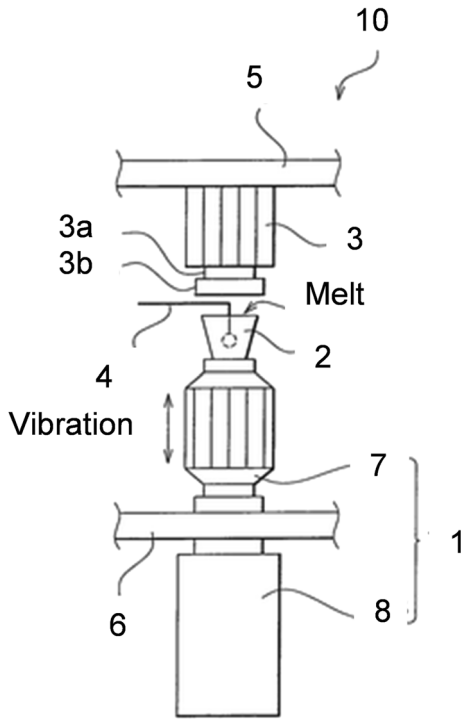

Fig. 13—Experimental setup for sono-solidification (10): 1—ultrasonic generator, 2—treatment vessel, 3—vessel holding device, 4—thermocouple, 5, 6—upper and lower plates, 7—ultrasonic horn, and 8—ultrasonic transducer. Reproduced from Ref. [176] with permission of US Government.

E. *Ultrasonic Treatment: Sono-Solidification*

Ultrasonic power is an effective and energy-efficient means to apply high shear and intense stress to liquids, powder–liquid mixtures, and slurries (Figure 13). This makes it a strong alternative to other stirring techniques, including high-shear mixers. A mechanism of melt stirring with ultrasound is the same as that described during degassing with the main role attributed to gas bubbles. In recent research,[94] direct observation was conducted of the penetration of a liquid metal into preexisting grooves (acting as microcapillary channels) during the ultrasonic processing of liquid Al-10 wt pct Cu alloy. This phenomenon is known as the sono-capillary or ultrasonic capillary effect. Some large-scale government programs are focused on researching the effect of ultrasonic treatment on solidification of alloys, in particular, the effect of ultrasonic vibration on the nucleation and growth of grains during solidification.[95]

The sonic or ultrasonic irradiation of molten metals is mainly carried out with magnetostrictive or piezoelectric transducers.[90] The coupling rods made of quartz, graphite, or various ceramic materials are used to transfer vibrations to a molten metal, and these materials are attached to the transducer by special cements. Due to a high temperature and corrosive environment, there are serious hardware challenges during service. For example, the oscillating rods, which are immersed into molten aluminum alloys, experience rapid dissolution causing detrimental performance effects. The rod material contaminates the melt, and the ultrasound distribution becomes nonuniform within the melt volume, intensifying cavitation near the transducer or the coupling rod face. Thus, the present designs are better suited for smaller volumes of molten alloys.

Ultrasound concepts were tested with many metals and alloys. Experiments of ultrasonic treatment during solidification of low-carbon steel showed, in addition to degassing, grain refinement and elimination of the Widmanstatten structure.[96] With ultrasonic treatment, pearlite was broken up and the average length of pearlite plates decreased several times. The most extensive research on ultrasound treatment was accumulated for aluminum alloys. For example, sono-solidification of Al alloys with Si content from 7 to 17 wt pct changed the shape and size of α-Al grains toward smaller and more regular ones.[97] The nonequilibrium α-Al grains contained higher Si content than the primary α-Al grains of the hypoeutectic Al-Si alloy, solidified without ultrasound treatment. In addition, the long plate-like, Fe-containing intermetallic phases were refined, contributing to an improvement in mechanical properties.

Experiments with the A356 alloy, treated during solidification with high-power ultrasound at a frequency of 18 kHz, showed superior microstructure characteristics with very low micro-porosity levels.[98] The effects included, in addition to a high level of hydrogen degassing, general microstructure refinement and positive morphological changes of eutectics. In turn, the ultrasonic treatment of AlSi7Mg and AlSi9Cu3 alloys allowed the achievement of a density of 98.5 pct after just 2 minutes, which affected the shape and size of the primary α-Al grains and the eutectic silicon. Similar to reports by other authors,[97] the ultrasound changed the morphology of Fe-containing intermetallic phases

$Al_{15}(Mn,Fe)_3Si_2$ and Al_5FeSi from long plates into short and thin particles with different shapes, uniformly distributed in the matrix.[99] The positive effects were also recorded for the 7050 aluminum alloy, having a different chemical composition than the previously described Al-Si casting grades. When solidified under the ultrasonic treatment, the alloy developed a finer microstructure than that obtained in the conventionally cast ingot with the α-Al phase changed from coarse rosette-like to fine globular morphology.[100] During postcasting heat treatment of such a microstructure, higher strengths were achieved after shorter homogenizing/aging periods, thus, reducing the energy consumption.

F. *Using Gas for Melt Stirring*

In conventional metallurgy, the treatment of molten metals with purged gases prior to casting is used to remove dissolved gases (particularly hydrogen), nonmetallic solid inclusions, and unwanted metallic impurities. For example, argon stirring of molten steel through porous plug is used to improve flotation of inclusions.[101] To accomplish melt purification, the equipment described earlier is used.[102] The new concepts of melt treatment use gas for agitation of the molten alloy to modify the solidification microstructure. So far, the same or slightly modified equipment is used for new applications. To implement the gas stirring concept, gas pumps were used for stirring molten metal directly in a melting furnace.[103] The purged gas improved the rate of melting through maintaining uniformity of composition and temperature in an otherwise standing volume of molten metal. In another design, the argon gas is delivered through metal tubes arranged in a spiral configuration in circumferentially spaced relation to one another in fixed position with respect to the refractory block.[104]

The use of gas bubbles to agitate a molten metal during solidification for a purpose of grain refinement through generating thixotropic slurries for rheocasting was introduced in 2006.[105,106] The essence of the apparatus is a porous graphite rod, with approximately 10 pct porosity, used as a diffuser (Figure 14). When mounted in a steel crucible and connected to an argon gas cylinder, it injects fine gas bubbles into the melt. A combination of rapid cooling and vigorous convection during solidification led to grain refinement in the A357 aluminum alloy. This method, called a gas-induced semisolid process was tested with the A356 alloy during sand casting.[107] A similar method, called rotating gas bubble stirring treatment, was found to be effective for magnesium alloys.[108] It relies on injecting fine gas bubbles into the melt during solidification through a rotating steel diffuser. As a result, fine and spherical α-Mg particles of the primary solid were obtained in an AZ91-2 wt pct Ca alloy. The formation of globular morphology was attributed to two phenomena: copious nucleation induced by cooling effect of gas bubbles and dendrite fragmentation, caused by stirring effect of bubbles.

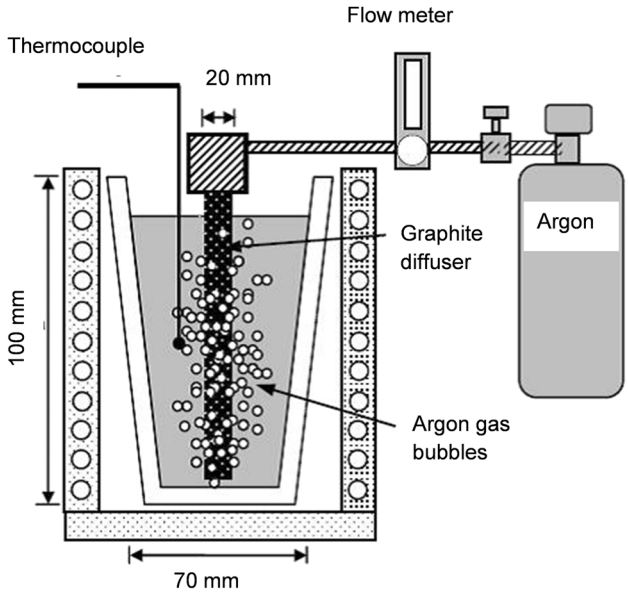

Fig. 14—Schematics of the apparatus used for grain refinement by melt mixing during solidification exploring gas bubbles purged by the porous graphite rod in the center. The porous graphite is used to purge gas with fine bubbles. Reproduced from Ref. [105] with permission of Elsevier.

G. *Role of Solid State Deformation Preceding Melting*

In previous sections, treatment was exclusively focused on a fully liquid state. Nevertheless, the nature of liquid alloy coexisting with solid, as is the case in the solidus–liquidus range, can also be controlled by a deformation history of its solid state prior to melting. The phenomenon is generally known as stress (or strain) induced melt activation (SIMA) and is classified as a route of generating globular structures for semisolid processing.[2] The full cycle involves four stages: casting, hot working, recrystallization, and partial melting. The term of RAP, developed as an acronym for the last two stages, exists in the literature as an equivalent to SIMA.[109]

The common techniques of imposing deformation include rolling,[110] extrusion,[111,112] and severe plastic deformation such as by equal channel angular pressing (ECAP).[113] A combination of hot rolling and ECAP was also found to generate a thixotropic microstructure in Mg-3 wt pct Zn alloy after reheating to a semisolid state.[114] Another combination explored to create thixotropic slurry is warm multiforging followed by recrystallization and partial melting. The method was tested for the 7175 aluminum alloy.[115] The SIMA mechanism is responsible for transformation of coarse metal particulates into thixotropic slurry during commercial-scale processing of metals within an injection molding barrel.[116,117] The limitation of SIMA is the maximum size of the component where cold deformation can be introduced. In practice, cross sections activated are rather small, for some deformation techniques below 30 mm.

VI. APPLICATION AREAS AND BENEFITS OF LME

The applications where LME can benefit the quality of cast components, described in this section, do not emphasize the conventional alloying, degassing, and melt purification.

A. *Casting Integrity*

Particular attention has been paid recently to so-called high integrity (or structural) castings, where after solidification, the net-shape parts have negligible porosity.[118] There are many factors affecting casting integrity in addition to alloy chemistry, including die/mold design, casting technique, and process parameters. An application of vibration during filling of thin wall investment castings, applied at sufficiently high temperature, increases metal fluidity. For the A356 aluminum alloy at temperatures exceeding 1023 K (750 °C), the fluidity increase reached 17 pct.[119] Similarly, a vibration during welding, seen as a widely accepted manufacturing procedure, led to grain refinement, improved weld integrity, and mechanical properties.[120] Substantial advantages are expected after application of LME to casting of fully molten alloys using the HPDC technique. The ability to achieve low porosity in predictable locations is seen as the major commercial gain in mass-scale production of net shape components. It is clear that the better quality components with higher strength lead to a series of savings due to the possibility of component size reduction for the same application causing lower material and energy consumption and a smaller machine needed to manufacture it translating to lower capital investment. The casting integrity is discussed further in a later section.

B. *Grain Refinement*

The grain size is seen as the primary feature describing the casting microstructure. For most alloys, grain refinement leads to an improvement of their structural homogeneity and mechanical properties. During conventional casting, the alloy grain size is affected by its chemical composition and by temperature of the molten state, temperature of the mold/die, and cooling rate.[121–123] Thus, the refined grain size is commonly seen as the benefit of LME. It should be emphasized that the grain size in cast structures may be interpreted differently than that in the wrought state. Therefore, to assess literature conclusions, it should be checked first what morphological feature was exactly measured. In some cases, a refinement is interpreted through a reduction of dendrites and quantified through secondary dendrite arm spacing. Also, a replacement of dendritic structures with globular ones is often seen as a refinement although a diameter of the primary solid particles may reach an order of 500 μm.

In a review performed in 1980 on the effects of vibration on solidification, theoretical models were assessed concluding a mechanical-fragmentation as a best fit for dendritically solidifying alloys.[124,125] For materials such as pure metals, solidifying with a planar front, a close correlation was revealed between the theoretical threshold for cavitation and the onset of grain refinement. No obvious evidence was found to suggest fundamental differences among ultrasonic, sonic, and subsonic vibration.

There are several ways that ultrasonic treatment alters grain nucleation. For example, the pressure oscillations in a melt under ultrasonic processing cause changes of the liquidus temperature. As a result, some parts of the melt are superheated and the other parts are undercooled. This phenomenon occurs at high frequencies and causes an increase in the amount of nuclei in the melt.[126,127]

According to theoretical mechanisms, cavitation leads to an increase in melting temperature predicted by the Clausius–Clapeyron equation:

$$\frac{\mathrm{d}P}{\mathrm{d}T} = \frac{L}{T\Delta v} = \frac{\Delta s}{\Delta v} \qquad [13]$$

where $\frac{\mathrm{d}P}{\mathrm{d}T}$ is the slope of the tangent to the coexistence curve at any point, L is the specific latent heat, T is the temperature, Δv is the specific volume change of the phase transition, and Δs is the specific entropy change of the phase transition. The Clausius–Clapeyron relation characterizes a discontinuous phase transition between two phases of matter of a single constituent. On a pressure–temperature (P–T) diagram, the line separating the two phases is known as the coexistence curve. The Clausius–Clapeyron relation gives the slope of the tangents to this curve. Thus, the temperature increase that is observed due to cavitation along wetting of otherwise unwetted insoluble particles and acting as nucleation substrates contributes to grain refinement.[128]

Ultrasonic treatments led to significant grain refinement of A356 alloy (Figure 15). The experimental verification revealed that ultrasonic treatment reduced the overall temperature of the treated melt, thus, reducing its pouring temperature.[128] It was subsequently concluded that the grain size of the A356 alloy was closely correlated with pouring temperature, suggesting that ultrasonic grain refinement is predominantly a result of heat removal by the horn and ultrasonic stirring.

C. *Exploring Melt Impurities for Grain Refinement*

Although this process relies on exploring exogenous particles for grain refinement similar to that discussed earlier, it is treated here separately because of its potentially great importance in practice. The essential point is to explore melt impurities as effective substrates for grain refinement. A particular role in grain refinement is ascribed to metallic oxides inevitably present in molten alloys, especially those with high reactivity to oxygen such as Mg and Al.[129,130] During melting, pouring, and transfer processes, as a result of melt turbulence, the oxide formed on the free surface is entrained into the alloy volume.[131] When the oxidized surface is folded over onto itself and entrained into the

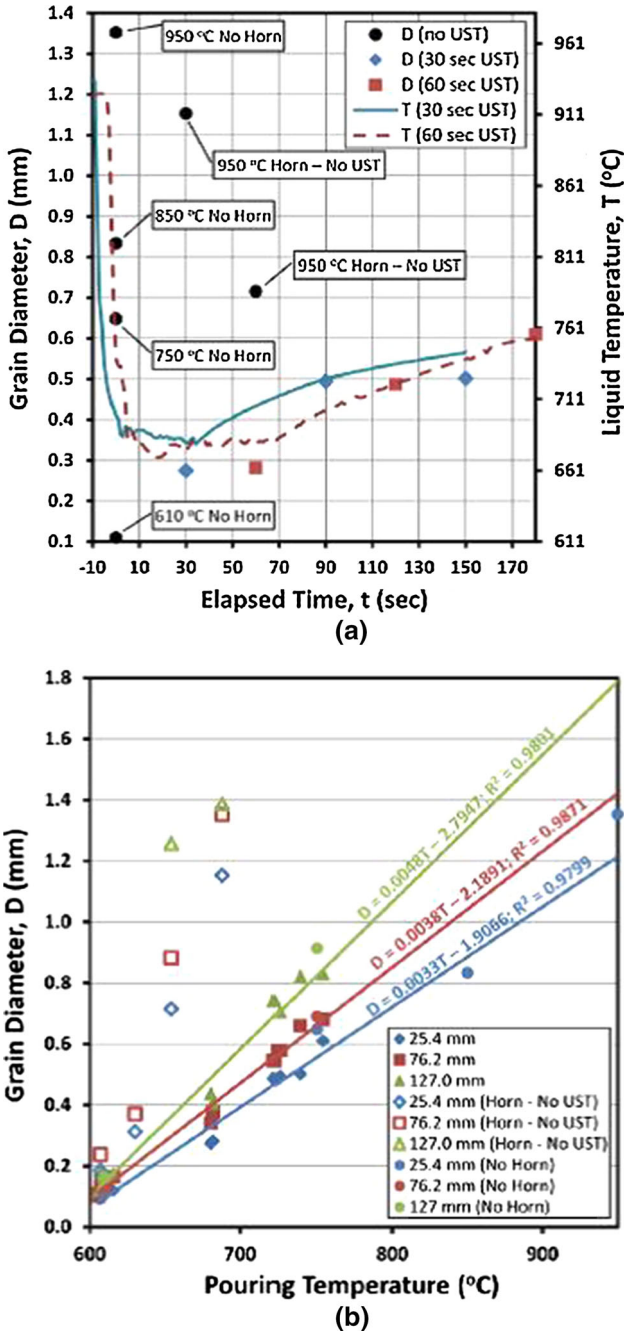

Fig. 15—Effect of ultrasonic treatment on grain size for cast A356 aluminum alloy: (*a*) variation of grain diameter at 25.4 mm from bottom of casting and liquid temperature with elapsed time at 1223 K (950 °C) for various ultrasonic treatments; (*b*) variation of grain diameter at 25.4, 76.2, and 127 mm from bottom of casting with pouring temperature. Reproduced from Ref. [128] with permission of MDPI, Basel, Switzerland.

bulk liquid, a particular case of defect is formed, called the double oxide film defect with characteristic features of unbonded oxide surfaces, separated by a gas. The entrained oxides along with other defects prevent manufacturing of high-integrity parts.

By exploring LME, the harmful effect of these oxide inclusions is not only eliminated but also used as the effective grain refiner. The oxide films on molten Mg alloys, when deliberately dispersed using intensive melt shearing, act as endogenous particles for effective grain refinement. For the Mg-9Al-1Zn alloy, the microscopic analysis of oxide, extracted from molten alloy, distinguished the submicrometer-size MgO particles, resulting from enforced breakup of the oxide films. High-resolution microscopy revealed good lattice matching between MgO and the α-Mg matrix.[132] The experiments conclude that by applying intensive melt shearing, the oxide films and the oxide particles are dispersed to the level that the rate of their agglomeration is slow, allowing casting and solidification to continue with the grain refining effect.

D. *Alloy Development*

It is generally known that vehicle lightweighting with aluminum alloys improves fuel economy and reduces emissions. In fact, it represents a complementary approach for hybrids and fuel cells to improve vehicle performance. The strategic visions to reduce the vehicle weight by up to 20 pct were not implemented, in part, due to barriers in appropriate alloys, especially for high-temperature applications and manufacturing technologies.[133] A development of new alloys with high-temperature capabilities and a high-volume, low-cost casting process will close the gap by allowing the production of high-integrity components. Such a technology would reduce component cost and increase competitiveness of the manufacturing industry.

The strengthening phases such as Al_2Cu, Mg_2Si, or Al_2CuMg within the Al-Si-Cu-Mg alloy usually coarsen or even dissolve at temperatures above 443 K (170 °C), thus, limiting their practical applications in engine blocks and cylinder heads. In a search for alloys with thermal stability exceeding 573 K (300 °C), alloying of the Al matrix with elements such as Ni, Fe, Cr, Ti, V, and Zr looks very promising.[134,135] Yet, these exotic elements having high melting temperatures generate extremely coarse compounds that deteriorate alloy properties in the as-cast state and require lengthy and costly postcasting homogenization treatment.[136–138] An example of coarse phases in an Al-Si-Cu-Mg base with Ti-V-Zr additions is shown in Figure 16. In some cases, even lengthy heat treatment is not effective. Moreover, to homogenize the molten alloy, high overheating and long holding times were required, leading to losses of other, more volatile constituents. It is believed, therefore, that the intensive physical treatment will allow not only for homogenizing its chemical composition but also for refining alloying compounds of complex chemistry, being in control of the alloy properties during service. The melt treatment during alloy generation should offer a number of benefits: (1) reducing the overheating temperature required during melting, (2) reducing the required holding time in a molten state, and (3) reducing holding times during postcast heat treatment or in some cases eliminate the need for heat treatment altogether, thus, essentially improving the energy effectiveness of the entire process.

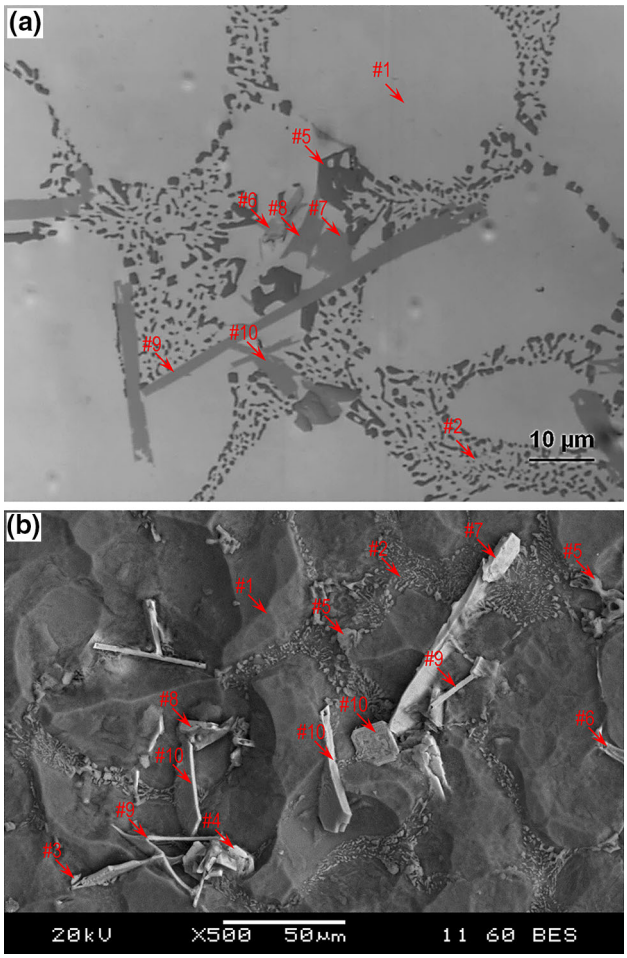

Fig. 16—Coarse phases requiring refinement *via* LME in the as-cast Al-Si-Cu-Mg alloy modified with Ti, V and Zr: (*a*) optical microscopy image; (*b*) SEM image after deep etching. Alloy composition: Si-7.02 pct, Cu-0.95 pct, Mg-0.48 pct, Zr-0.56 pct, Ti-0.20 pct, V-0.32 pct. Composition of phases marked, based on EDX analysis: #1 α-aluminum, #2 Eutectic silicon, #3 Al2.1Cu, #4 Al8.5Si2.4Cu,#5 Al7.2Si8.3Cu2Mg6.9, #6 Al14Si7.1FeMg3.3, #7 Al2.8Si3.8V1.6Zr, #8 Al5.1Si35.4Ti1.6Zr5.7Fe, #9 Al21.4Si4.1Ti3.5VZr3.9, #10 Al6.7-Si1.2TiZr1.8. All values are in wt pct. Reproduced from Ref. [177] with permission of Elsevier.

E. *Semisolid State Technologies*

Semisolid processing has been initially seen as the technology capable of manufacturing net shape components at low cost with properties substantially better than that offered by casting. The primary objective of LME within all semisolid technologies is to generate thixotropic structures through nucleation of globular forms instead of dendritic ones during solidification to essentially improve flow during net shape forming and bringing several other benefits.[139]

1. *Role of Temperature and Time*

Lowering the processing temperature below the liquidus replaces the molten alloy with semisolid slurry. Although in casting of fully molten alloys the LME provides general improvements of melt quality through refining and degassing, in semisolid processing, it aims additionally at the generation of globular morphologies of the primary solid. In alloys with multiphase composition, in addition to the matrix, also the other phases experience modification.

To assess the role of temperature, high-intensity ultrasonic melt treatment was applied to an Al-0.4 wt pct Ti alloy over three temperature ranges: 1083 K to 1043 K (810 °C to 770 °C) (above liquidus), 1043 K to 1003 K (770 °C to 730 °C) (across liquidus), and 1003 K to 963 K (730 °C to 690 °C) (below liquidus).[140] As a result of ultrasonication, the primary Al_3Ti intermetallics were refined over all three temperature ranges and their morphology changed from typical large dendritic plates to small compact tablets. As shown in Figure 17, the ultrasonication effect depends on processing temperature.

A need for deeper understanding of formation of thixotropic structures was pointed out recently through research showing an importance of time over melt temperature during processing emphasizing the importance of melting kinetics.[141] The experiments conducted with high-purity aluminum and the binary Al-Si eutectic alloy claim the possibility of forming thixotropic structures in materials with no practical freezing range being at odds with the conventional requirement of the freezing range defined by inspecting the liquid fraction *vs* temperature curve and defined as the processing window. The results suggest that the time sensitivity depends on the sample mass, the heat flux, and the phase transformation temperature.

2. *Executing LME Within Solidus–Liquidus Range*

The initial research of semisolid processing involved rheocasting where the molten alloy treatment during cooling to the liquidus–solidus range caused transformations from dendritic to globular morphologies. As technology progressed, several liquid metal treatments aimed at generating globular morphologies were introduced. Semisolid processing was subsequently dominated by thixoforming (thixocasting, thixoforging) where thixotropic raw material, created during the first stage, was subsequently reheated to semisolid range and then subjected to net shape forming. Nevertheless, due to excessive cost, thixocasting soon lost its advantage and today's semisolid processing is again dominated by rheo-routes.

In contrast to dendritic forms, thixotropic mixtures act as deformable semicohesive spheroidal solids saturated with liquid where a macroscopic stress applied is carried by both the solid and liquid phases (Figure 18(a)). This deformation behavior is unique for thixotropic structures. Alloys with dendritic features cannot be deformed by grain rearrangement due to significant geometric interference of complex shape solid features, leading to high flow resistance in semisolid state. To exhibit thixotropic properties, spheroidal particles should be surrounded by the liquid matrix and separated from each other. Yet, solid particles may often be interconnected forming complex conglomerates. The particle agglomeration, as shown in Figures 18(b) through (d), is detrimental to flow behavior of the semisolid slurry. This explains challenges of LME to

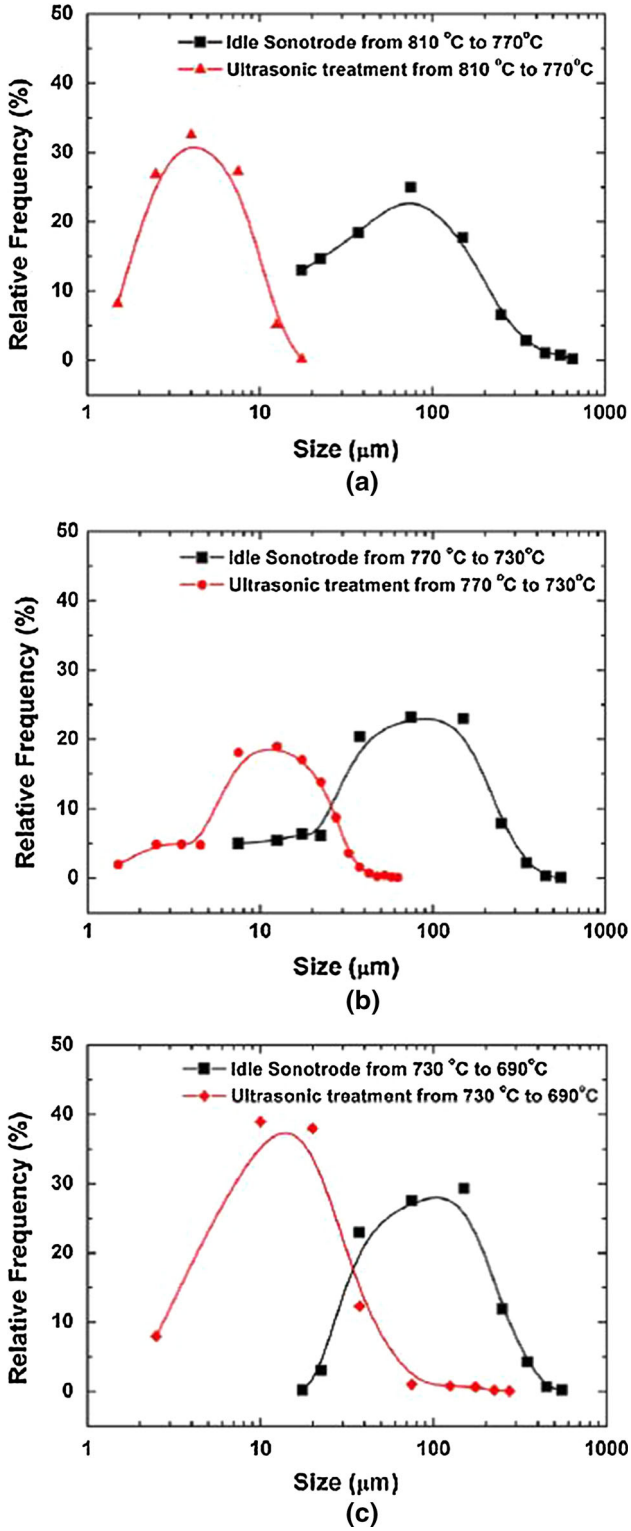

Fig. 17—Measurements of the primary Al_3Ti particle size distribution within the ingot samples after ultrasonic treatment (*a*) treatment performed from 1083 K to 1043 K (810 °C to 770 °C); (*b*) treatment performed from 1043 K to 1003 K (770 °C to 730 °C); (*c*) treatment performed from 1003 K to 963 K (730 °C to 690 °C). Reproduced from Ref. [140] with permission of Elsevier.

eliminate conglomerates and generate the optimum thixotropic morphologies.

Although during rheocasting the physical treatment starts within a single-phase liquid, it is continued during coexistence of two-phase thixotropic slurry (Figure 19). As a result, at the time of net shape forming, only a portion of metal remains liquid and requires attention. The solid fraction range allowing processing was initially defined between 5 and 60 pct with the upper limit seen as a content above which alloy freezes so it could not been flown into the mold cavity. Nevertheless, after semisolid extrusion molding was invented, that limit was substantially raised up to over 85 pct, meaning that only a small fraction of liquid metal remained at the time of net shape forming.[142,143] To add complexity, the thixoforming path involves partial remelting of previously solidified thixotropic alloy, just creating within it again a fraction of fresh liquid. It should be emphasized that the chemical composition of the liquid fraction in semisolid state differs from that measured for the bulk alloy, and as temperature decreases, these differences grow. To take advantage of having melts with two different compositions, *i.e.,* initial one and at the stage of forming, the overall alloy chemistry should specifically be designed for this purpose.[144] In addition to less challenging alloys from the hardware perspective such as Al and Mg grades, there are also attempts to process alloys with higher melting temperatures including steel.[145–147] A lack of specifically designed alloys for this technology is seen as one of the obstacles contributing to still limited commercialization of semisolid processing.

F. *Near-Liquidus Forming*

At the time when rheocasting was invented, the formation of globular structures was explained through "breaking up dendrites" during the freezing process either by mechanical stirring or *via* other forms of agitation. In the next step, fragments of dendrites within the melt volume would act as nuclei of new grains that transform to spheroids. Nevertheless, experimental evidence accumulated later seriously questioned this mechanism. Direct observations of the solidification of transparent liquids with metal-like crystallization characteristics and numerical modeling suggest rather that globular crystals form through direct nucleation from a liquid instead of from fragments of broken dendrites.[148]

As explained earlier, the morphology of solid in the two-phase mixture of solid and liquid is controlled by cooling, convection, or their combination. The particular role in generating globular forms, however, is associated with the melt temperature.[149–151] It is a general casting observation that lowering the pouring temperature promotes the formation of equiaxed solidification morphologies. In particular, when superheating is sufficiently low, the whole melt is undercooled and copious heterogeneous nucleation takes place throughout it. This leads to complete elimination of the

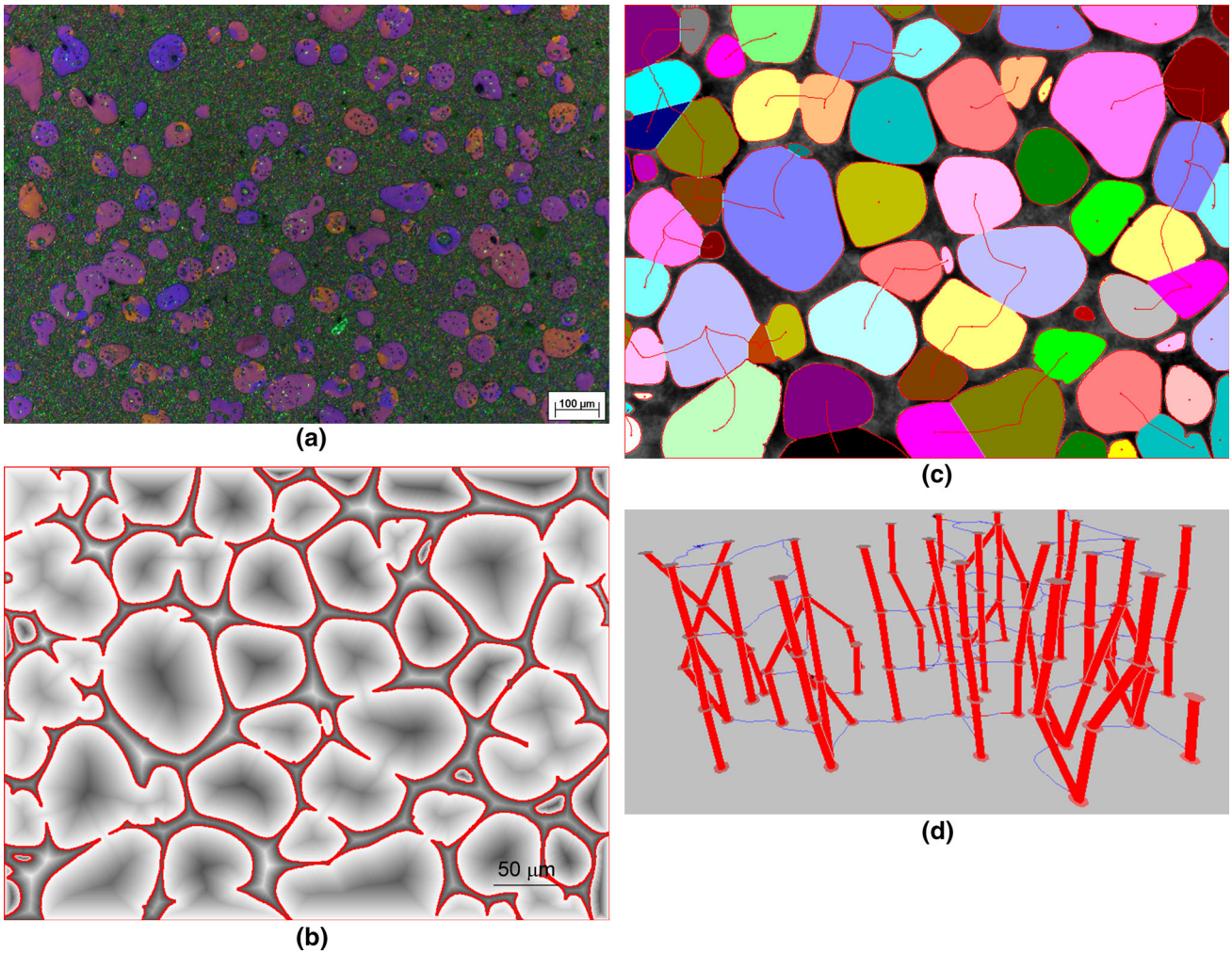

Fig. 18—Globular morphology generated during semisolid processing and revealing formation of conglomerates between solid particles by metallographic technique of reconstructing the 3D space connections of particles, described in Ref. [178]: (*a*) Mg-9 pct Al-1 pct Zn (wt pct) alloy processed by injection molding: (*b*) Euclidean distance map of the grains created for determination of topological characteristics; (*c*) 2D skeleton separating the touching grains used for 3D structure reconstructions; (*d*) skeleton in 3D formed by connecting the ultimate eroded points of 2D sections. (b) through (d) reproduced from Ref. [178] with permission of Prof. A. Kazakov.

columnar zone and to the formation of fine equiaxed grains in the entire melt volume. It is clear that the temperature control imposed by the near liquidus process may be challenging for certain hardware and larger alloy volumes. A combination of melt shearing with reciprocating injection screw and precise temperature control in near liquidus range conducted within the injection molding machine led to an ultrafine microstructure (Figure 20). For magnesium alloy AZ91D, this way of processing led to a superior combination of strength and ductility.[149] Electromagnetic stirring at near liquidus temperatures was explored for the thixotropic structure of AZ91D alloy.[87] Near liquidus processing combined with squeeze casting was found beneficial for aluminum alloy as well.[152]

G. *Alloy Generation by Mixing Thixotropic Slurries*

Mixing of thixotropic slurries represents a novel technique of alloy generation.[153] A selection of chemistry of individual slurries, mixing proportions, and preheating temperature allows controlling partition of alloying elements between the solid and liquid, thus, generating alloys with unique microstructures, essentially different from those formed after the conventional mixing of completely molten ingredients. The same result may be achieved by mixing solid particulates (activated by cold deformation) of different alloys followed by partial remelting.[6]

The concept of alloy formation during the semisolid mixing of two alloys of the same elements is shown in Figure 21 along with the simple phase diagram and accompanying room temperature microstructures. When alloy 1 enters the semisolid state, the melting of alloy 2 is already well advanced. As a consequence, the predominant portion of the liquid phase, which is rich in B, is derived from alloy 2. For the two alloys considered here, at all molding temperatures, alloy 1 contributes more solids while alloy 2 supplies more liquid. With increasing the preheating temperature, the B content in the liquid is reduced due to a dissolution of the solid phase rich in A.

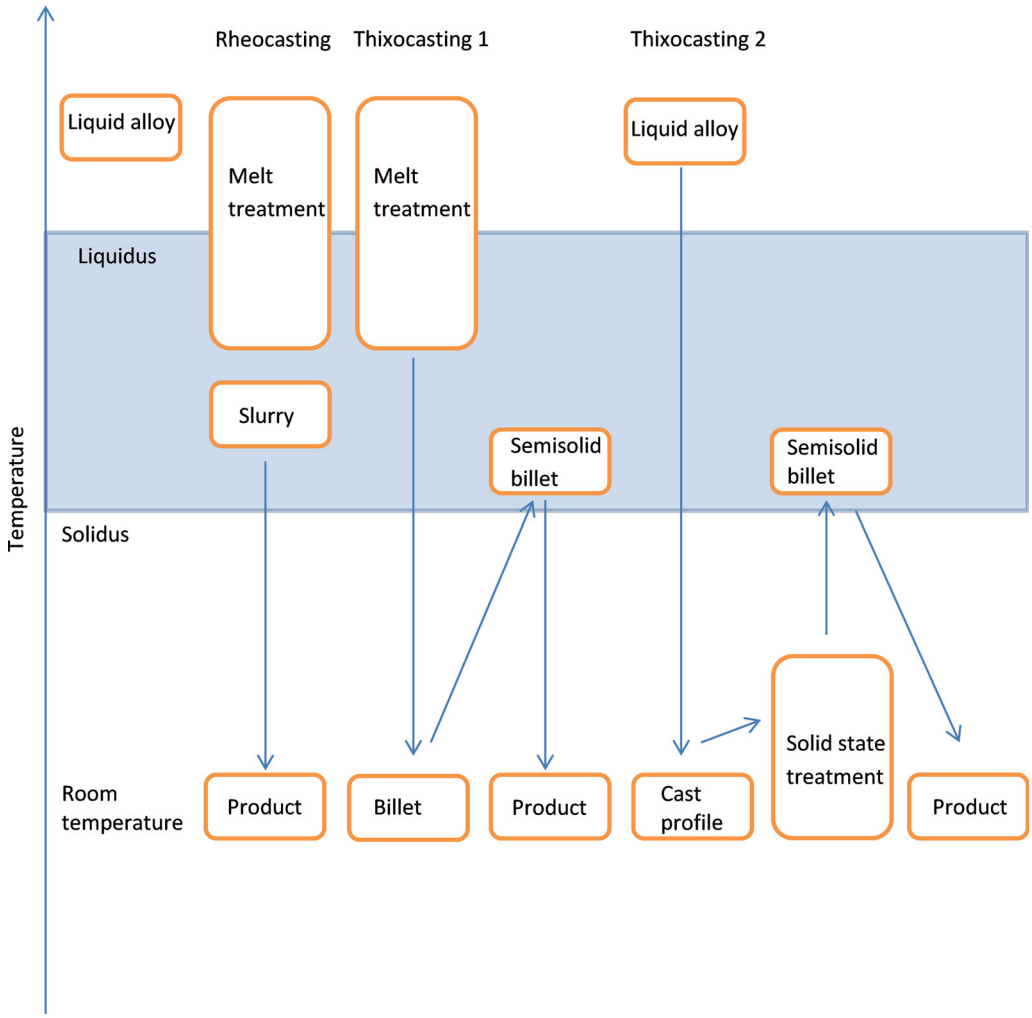

Fig. 19—Schematics explaining concepts of metal treatment during semisolid processing based on rheo- and thixo-routes. Reproduced from Ref. [179] with permission of NADCA.

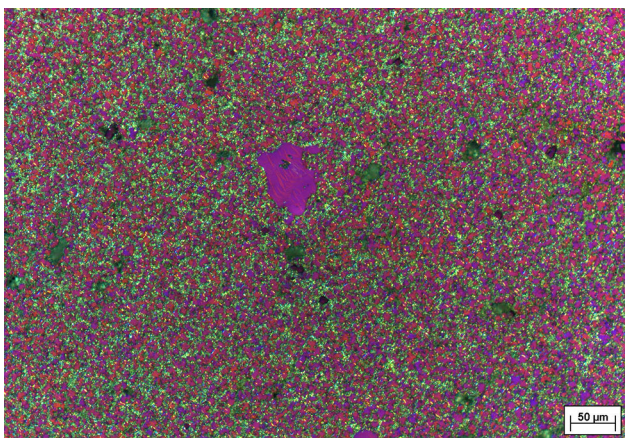

Fig. 20—Near liquidus processing: fine-grain microstructure with a single unmelted particle shown in the center. Magnesium alloy Mg-9 pct Al-1 pct Zn (wt pct): color etching revealing approximate grain orientations.

The alloy generation by mixing thixotropic slurries during semisolid injection molding is of great engineering importance. The potential advantages may be shown by considering mixing of several commercial alloys where each of them was designed for different properties: Mg-6Al, Mg-5Al-2Sr, Mg-2Ce-0.3Zn and Mg-9Al-1Zn.[2] Although Mg-9Al-1Zn shows good mechanical properties with excellent castability, the Mg-6Al is known for its high ductility and toughness. Hence, by mixing these two grades, an intermediate range of properties may be covered. Then, the Mg-5Al-2Sr alloy has excellent creep resistance at high temperatures. An increase in Al content during alloying with Mg-9Al-1Zn improves its castability and room temperature strength while still preserving satisfactory creep resistance at moderate temperatures. Similarly, the alloy Mg-2Ce-0.3Zn is designed for high-creep resistance. An absence of Al results in reduced tensile properties at room temperature and demanding casting behavior. Combining it with Mg-9Al-1Zn could allow for balancing among alloy castability, room temperature yield, tensile strength, and creep resistance.

H. *Mixing Immiscible Metals*

There are many couples of metals where the two elements exhibit a positive heat of mixing (positive ΔH).

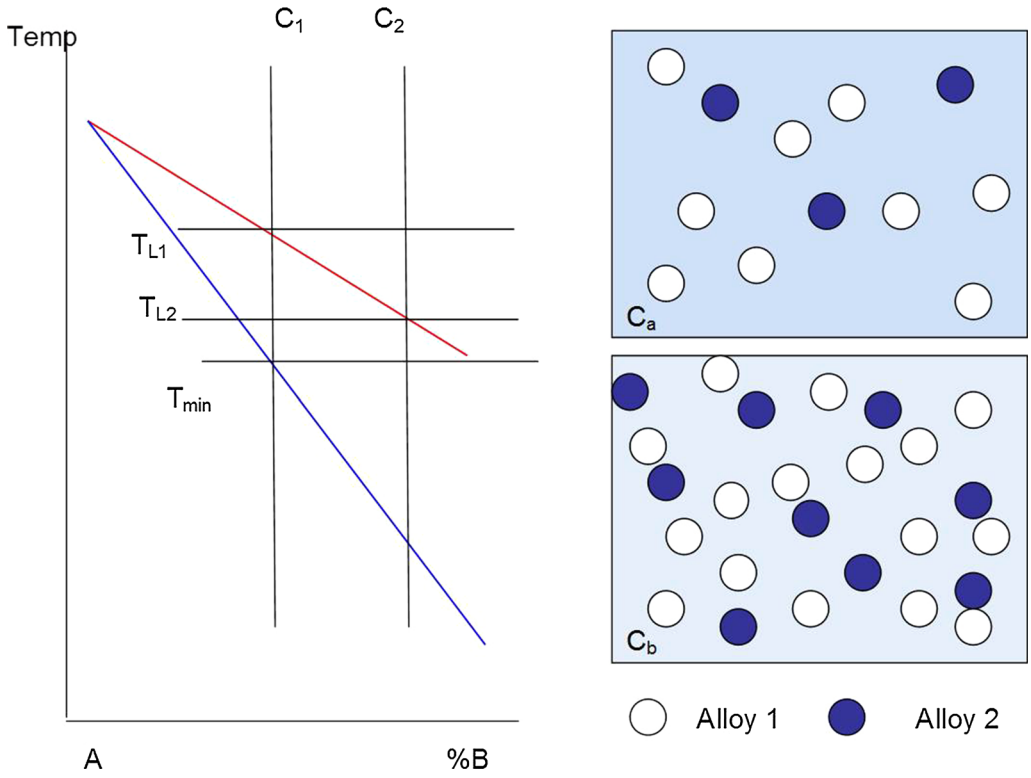

Fig. 21—Concept of alloy generation by mixing thixotropic slurries: alloy 1 and 2 of the same components A and B were mixed together. C_1 and C_2 show their phase composition at two different temperatures.

As a result, they are unable to form alloys with each other; *i.e.*, the binary phase diagrams show a miscibility gap that represents the equilibrium between two liquids of different compositions. Examples include Cu-Ta, Fe-Ag, Al-Ta, Pb-Al, Zn-Pb, Pt-Pd, Cu-Pd, Al-Bi, Al-In, Al-Pb, Ga-Pb, Pb-Zn-Sn, Al-Pb, and Cu-Pb. To overcome this obvious challenge, several methods were proposed. In some techniques, stress is applied to the liquid phase with some analogy to the observation from the solid state known as the deformation-induced (severe plastic deformation) intermixing of equilibrium immiscible elements, leading in stressed diffusion couples to the homogeneous microstructure.[154]

The technique developed in the 1980s at MIT,[155] called the "Mixalloying Process," explores two or more molten liquid reservoirs and connecting pipes to pump alloys and injecting them through nozzles to the mixing chamber. In the chamber, two liquid metal jets were impinged into a mixing head and intimately mixed the ingredients by turbulence. After mixing, the alloy is cast to a water-cooled copper mold. Using this technique, dispersed-phase microstructures of the immiscible Pb-Zn, Pb-Zn-Sn, and Pb-Al alloys were produced.[156,157]

Another technique is based on shear mixing semisolid slurries.[8] In the first step, the initial stabilization is achieved by applying an intensive shear stress–strain field to create a fine homogeneous liquid dispersion at a temperature above T_M. In the second step, a fine liquid dispersion is further stabilized by shearing it at a temperature below T_M to create a semisolid slurry, the viscosity of which is high enough that both Stokes and Marangoni motions can no longer produce coarse separation. The high-pressure torsion was explored for bulk mechanical alloying of combinations of immiscible Ag-Ni and Nb-Zr systems.[158] For Ag and Ni, no alloying on an atomic scale was observed after 100 rotations. In contrast, the β-Zr phase appeared after two rotations in the Nb-Zr system. Furthermore, Nb and Zr were completely mixed to form a bcc structured single phase after 100 rotations. Nonequilibrium phases can form as a result of high-pressure torsion. Another strategy for the generation of a new metastable alloy of immiscible metals is by the pulsed laser irradiation of colloidal nanoparticles.[159] Using this technique, $Au_{1-x}Ni_x$ 3D structures with 56 at pct of Ni in Au were successfully manufactured.

I. *Mixing Molten Alloys to Generate Thixotropic Slurries*

Manipulating two liquid alloys is used in the continuous rheo-conversion process developed at MPI/WPI in 2002.[160] The process is based on a passive mixing of two liquids of equal or different compositions in which the nucleation and growth of the primary phase are controlled using a specially designed "reactor" providing heat extraction, copious nucleation, and forced convection during the initial stage of solidification. As a result, globular structures are formed. Variable heat extraction rates can be obtained by controlling either the superheat of the melt, the temperature of the channel system, or the temperature of the reactor. The technique

has been applied in both hyper-eutectic Al-Si alloys (*i.e.*, A390) and hypo-eutectic Al-Si alloys (A356, A357)

J. *Metal Matrix Composites*

Although benefits of metal matrix composites are well established, there are still issues with a technology to manufacture bulk quantities with uniform distribution of reinforcement, especially of the nanometer range. The LME techniques provide manufacturing opportunities of metal matrix composites by exploring (1) processes with the matrix in the liquid state and (2) processes with the matrix in the semisolid state or combinations of both routes. Examples of technologies used include mechanical stir casting[161] and injection molding or casting with intensive melt shearing.[162] In the latter example, intensive shearing in a twin screw barrel helped to break up the agglomerates and uniformly dispersed the particles within the melt. It is claimed that high shear rate and shorter cycle time are beneficial. A shear form imposed by injection screw was found beneficial with generating composites with semisolid metallic matrix reinforced by both the inert or reactive particles.[163]

The ultrasonic cavitation-assisted processing was also found to be an effective route for composite manufacturing. Positive results were obtained for Al_2O_3 and SiC nanoparticles and the A356 base where particles were dispersed in molten metal by ultrasonic cavitation and acoustic streaming technology to avoid agglomeration and coalescence.[164] As a result, the microstructure was refined and tensile strength, yield strength, and elongation increased significantly. A limitation was recorded on ensuring proper cavitation and acoustic streaming in sufficient melt volume for efficient dispersion of the nanoparticles. The same ultrasonic cavitation-assisted casting process was used to fabricate the aluminum alloy-nano boron carbide metal matrix nanocomposites.[165] A combination of stir casting and ultrasonic vibration with a frequency of 18 to 24 Hz was found to have a positive effect on nanoparticle distribution within the composite.[166]

K. *Generating Metallic Foams*

Metallic foams and porous metals are materials that contain in their structure deliberately created pores. Solid metallic foams are known for their interesting combinations of physical and mechanical properties such as high stiffness accompanied by very low specific weight or high compression strengths. There is some confusion in distinguishing metallic foams from cellular metals, porous metals, and metal sponges.[167] The production methods of metallic foams rely on creating gas bubbles in the liquid either by gas injection or by decomposing a chemical blowing agent in the melt.

Aluminum foams are very useful and promising functional materials with special advantages such as good heat resistance, sound and heat absorption, high strength, and easy recycling. On several manufacturing methods, the gas injection where foams can be produced continuously looks promising.[168] To generate foam, air

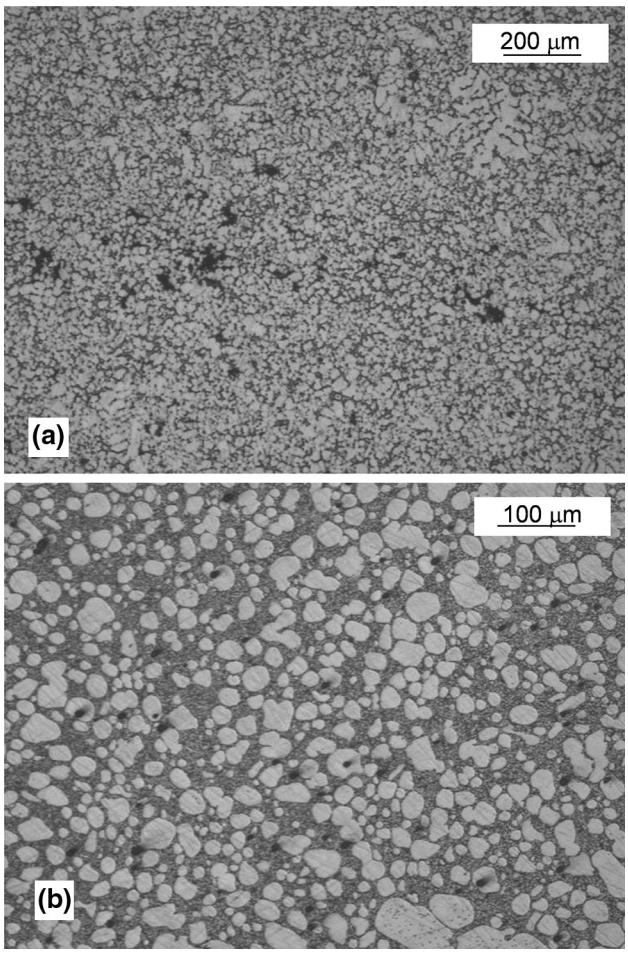

Fig. 22—Comparison of microstructure after casting of completely molten alloy resulting in dendritic morphology and some porosity (*a*) with that after semisolid processing showing globular morphologies with no porosity (*b*). Magnesium-based alloy. Reproduced from Ref. [179] with permission of NADCA.

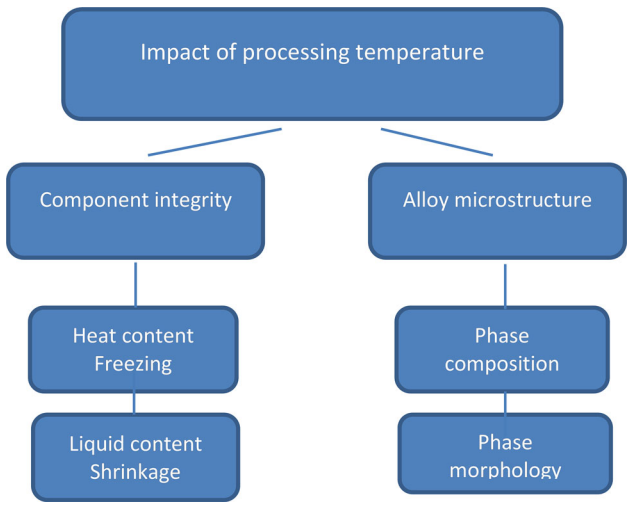

Fig. 23—Influence of temperature during semisolid processing on component integrity and microstructure. Reproduced from Ref. [179] with permission of NADCA.

is injected through a nozzle into molten aluminum composites, forming a liquid foam body, which is stabilized by the presence of solid ceramic particles at gas–liquid interfaces of the cell walls.[169] The major advantage of metal foams produced by casting over other methods is the shell-like skin at the outer surface and the mostly closed cell foam inside the structure.[170] As a separate family, foams with thixotropic structure of the metallic skeleton may be generated.[10] Although details depend on a particular production method, there are great opportunities in exploring LME in all of them.[171,172]

VII. ASSESSING THE EFFECT OF MELT TREATMENT ON PRODUCT QUALITY

When considering casting from temperatures exceeding liquidus, LME has a universally positive effect on the part quality through improving the part integrity, alloy purity, and refining microstructure. During other processes such as composite manufacturing, alloys with exotic ingredients improving homogeneity through LME are also straightforward to understand. The issue is becoming more complex when applying LME to alloys at temperatures of the liquidus–solidus range.

Nevertheless, several benefits were associated with formation of fine equiaxed morphologies instead of coarse dendritic structures (Figure 22). The most frequently quoted include improved metal fluidity, refined and uniformly dispersed porosity, finer second phases, improved resistance to hot tearing, longer fatigue life, and greater pressure tightness.[173] Yet, in the literature, the component integrity and alloy microstructure are often not separated, the mechanism of improvement is difficult to assess.

The term ''nondendritic structures'' typically covers numerous changes within both (1) the alloy microstructure and (2) the part integrity (Figure 23). Thus, to assess the influence of LME on component properties, the factors affecting its performance must be distinguished.[2] First, the transition from casting using molten metal into semisolid slurry reduces liquid content resulting in lower solidification shrinkage. Then, the thixotropic nature of the slurry improves flow during filling the die/mold cavity causing reduction of defects especially for parts with intricate shapes, having complex filling paths. Both factors improve the part internal integrity and have a positive effect on part quality. At the same time, the reduced temperature of semisolid slurry increases the tendency to premature freezing preventing complete part cavity filling, which is seen as a negative factor. The effect of processing temperature on alloy microstructure is not straightforward. The alloy microstructure consists of phases with specific size and morphologies, and a replacement of dendritic forms with globular ones is not seen as exerting a universally positive influence on properties. In fact, a presence of coarse globules of the primary solid leads to reduced strength.[174] Also, the liquid phase solidified at the end, being highly enriched in alloying elements, can have a brittle nature and therefore lead to reduction of overall ductility. In contrast, the microstructure refinement achieved by LME has a positive effect on part properties for all solidification morphologies: dendritic, globular, and equiaxed.

VIII. SUMMARY

To address the needs of our modern manufacturing industry, there is a search for novel technologies for large-scale production of net shape components having high performance. Techniques based on net shape forming directly from the liquid state, like HPDC, offer substantial advantages in terms of manufacturing simplicity, cost, and energy consumption over complex multistep processes based on solid state forming. An alternative manufacturing route exploring semisolid processing generated high expectations but, after several decades of research, still did not pass the critical breakthrough. Engineering molten alloys to influence their solidification process, leading to increasing the component performance characteristics through improving its integrity and alloy microstructure, looks very promising but is still not fully explored. Recent global developments indicate that exploring the synergy of melt chemistry and physical treatments achieved through LME allows the creation of the optimum conditions for nucleation and growth during solidification, positively affecting quality of castings.

REFERENCES

1. K.C. John: *Metal Casting and Joining*, Delhi, PHI Learning, 2015, pp. 3–13.
2. F. Czerwinski: *Magnesium Injection Molding*, Springer, New York, 2008, pp. 81–110.
3. E.J. Vinarcik: *High Integrity Die Casting*, Wiley, New York, 2004, pp. 3–16.
4. F. Czerwinski: *Adv. Mater. Process.*, 2016, vol. 174 (9).
5. I. Brodova, P. Popel, and G. Eskin: *Liquid Metal Processing—Applications to Aluminum Alloy Production*, Taylor & Francis, London, 2002, p. 147.
6. F. Czerwinski, R. Domodossola, G. Mariconda, and D. Smith: US Patent 7,694,715, April 13, 2010.
7. D. Apelian, Q. Pan, and M. Findon: *Die Cast. Eng.*, 2004, vol. 48, pp. 22–28.
8. Z. Fan, S. Ji, and J. Zhang: *Mater. Sci. Technol.*, 2001, vol. 17, pp. 837–42.
9. G. Yan, S. Zhao, S. Ma, and H. Shou: *Mater. Charact.*, 2012, vol. 69, pp. 45–51.
10. F. Czerwinski: US Patent 7,699,092, April 20, 2010.
11. W. Marten: *Thermowell Failure at Sodium Components Test Investigation*, US Atomic Energy Commission Technical Data Record, 1973, pp. 4–37.
12. S. Moriya: *Proceedings of Fourth International Conference on Liquid Metal Engineering and Technology*, Avignion, France, 1988.
13. R. Hall: *Nucl. Energ.*, 1985, vol. 24 (3), pp. 145–49.
14. Organization site: Liquid Metal Technology Inc., http://liquidmetal.com. Accessed May 2, 2016.
15. J. Dantzig and M. Rappaz: *Solidification*, CRC Press, Boca Raton, 2009, pp. 151–90.
16. B. Chalmers: *Principles of Solidification*, Wiley, London, 1964.
17. M.W.A. Volmer: *Physikal. Chemie (Leipzig)*, 1925, vol. 119, p. 277.

18. G. Sosso, J. Chen, S. Coox, M. Fitzner, P. Pedevilla, A. Zen, and A. Michaelides: *Chem. Rev.*, 2016, vol. 116, pp. 7078–116.
19. T. Kawasaki and H. Tanaka: *Proc. Natl. Acad. Sci. USA*, 2010, vol. 107 (32), pp. 14036–41.
20. T. Quested and A. Greer: *Acta Mater.*, 2005, vol. 53 (9), pp. 2683–92.
21. Z. Fan: *Metall. Mater. Trans. A*, 2013, vol. 44A, pp. 1409–18.
22. C. Wang and C. Beckermann: *Metall. Trans. A*, 1993, vol. 24A, pp. 2787–802.
23. B. Levich and D. Spalding: *Int. J. Phys. Chem. Hydrodyn.*, 1981, vol. 2 (4), pp. 237–357.
24. J. Pilling and A. Hellawell: *Metall. Mater. Trans. A*, 1996, vol. 27A, pp. 229–32.
25. K. Deagnevski, A. Mullins, D. Walker, and R. Cochrane: *Acta Mater.*, 2002, vol. 50, pp. 3743–55.
26. N. Iqbal, N. Van Dijk, S. Offerman, M. Moret, L. Katgerman, and G. Kearly: *Acta Mater.*, 2005, vol. 53, pp. 2875–80.
27. W. Burgmann, T. Gustsfson, and J. Davene: *Metall. Res. Technol.*, 2014, vol. 111 (2), pp. 119–28.
28. D. Neff: *Modern Cast.*, 2002, vol. 5, pp. 1–4.
29. R. Gottschalk: US Patent 3,159,478, 1 12 1964.
30. P. Le Brun and A. Mathis: *Light Metals*, Ed. A.T. Tabereaux, TMS, Warrendale, 2004.
31. R. Kendrick, G. Muneratti, S. Consoli, F. Voltazz, and S. Barison: *Metall. Sci. Technol.*, 2012, vols. 30–2, pp. 3–11.
32. R. Simon and P. Careil: *Granular and Powder Fluxes for Aluminum Alloys, Cleaning Efficiency, Cost and Environmental Aspects*, Foseco Foundry Practice, 2012, p. 247.
33. S. Simmons: *Aluminium Insight*, 2016, vol. 10 (1), pp. 1–2.
34. Online document: *The most efficient alkali and inclusion removal technology in aluminium casthouse furnaces, STAS*, http://www.stas.com/en/rfi-rotary-flux-injector.html. Accessed 5 May 2016.
35. A. Pascual: *China Foundry*, 2009, vol. 6 (4), pp. 358–65.
36. G. Eskin: *Ultrason. Sonochem.*, 1995, vol. 2 (2), pp. S137–41.
37. J. Bang and K. Suslick: *Adv. Mater.*, 2010, vol. 22, pp. 1039–59.
38. J. Li, T. Momono, Y. Tayu, and Y. Fu: *Mater. Lett.*, 2008, vol. 62 (25), pp. 4152–54.
39. N. Alba-Baena and D. Eskin: *Light Metals 2013,* B. Sadler ed., TMS, Warrendale, PA, 2013.
40. T. Meek, Q. Han, and H. Xu: *Degassing of Aluminum Alloys Using Ultrasonic Vibration*, Oak Ridge National Laboratory, Report ORNL/TM-2006/61, 2006, pp. 9–34.
41. V. Rundguist: US Patent Application 20150135901, May 21, 2015.
42. H. Puga, J. Texeira, J. Barbosa, E. Seabra, S. Ribeiro, and M. Prokic: *Mater. Lett.*, 2009, vol. 63, pp. 2089–92.
43. H. Puga, J. Barbosa, E. Seabra, S. Ribeiro, and M. Prokic: *Mater. Lett.*, 2009, vol. 63 (9–10), pp. 806–08.
44. H. Puga, J. Barbosa, N. Tuan, and F. Silva: *Trans. Nonferrous Met. Soc. China*, 2014, vol. 24, pp. 3459–64.
45. V. Rundquist and K. Gill: US Patent Application 20111247456A1, October 13, 2011.
46. Online document: *Ultrasound Treatment Removes Hydrogen from Molten Aluminum*, ASM Internationa, 10 12 2014, http://www.asminternational.org. Accessed 30 May 2016.
47. S. Bell, B. Davis, A. Javaid, and E. Essadiqi: *Final Report on Refining Technologies of Aluminum*, Natural Resources Canada, Report No. 2003-21(CF), Ottawa, 2003, pp. 2–12.
48. I.A. Andrews and A.L. Matthews: *Ductile Iron News*, 1999, vol. 1, pp. 1–7.
49. J. Hitchings: *INCAST Magazine*, 2012, vol. 05, pp. 24–27.
50. Online document: *Ceramic Honeycomb-Molten Metal Filtration*, http://www.induceramic.com. Accessed May 26, 2016.
51. Online document: *Ceramic Foam Filter Molten Metal Filtration*, http://www.induceramic.com. Accessed May 26, 2016.
52. M. Tucker and J. Tu: *Int. J. Appl. Ceram. Technol.*, 2012, pp. 1–7.
53. A. Leonov and N. Dechko: *Refract. Ind. Ceram.*, 1999, vol. 40 (11), pp. 537–42.
54. Z. Taslicukur, C. Balaban, and N. Kuskonmaz: *J. Eur. Ceram. Soc.*, 2007, vol. 27, nos. 2, 3, pp. 637–40.
55. S. Bao: Ph.D. Dissertation, Norwegian University of Science and Technology, Trondheim, 2011.
56. N. Sobczak, J. Sobczak, R. Asthana, and R. Purgert: *China Foundry*, 2010, vol. 7 (4), pp. 425–37.
57. E. Bagherian, M. Ariffin, and S. Sulaiman: *Int. J. Pure Appl. Res. Eng. Technol.*, 2015, vol. 4, no. 3, pp. 27–43.
58. K. Janiszewski: *Refining of Liquid Steel from Nonmetallic Inclusions by Filtration*, Poland Slask Publisher, Katowice, 2012.
59. B. Lipowska, J. Witek, T. Wala, A. Karwinski, P. Wieliczko, M. Aslamowicz, and A. Oscilowski: *Archiv. Foundry Eng.*, 2014, vol. 14 (4), pp. 61–66.
60. H. Bali: WO Patent 2003020660 A1, March 13, 2003.
61. K. Juma: US Patent 7,963,402, June 21, 2011.
62. G. Eskin and D. Eskin: *Ultrasonic Treatment of Light Alloy Melts*, CRC Press, Boca Raton, 2015.
63. D. Chernov: *Zapiski Imperat. Russ. Technich. Obshch.*, 1879, vol. 1, pp. 1–24.
64. M. Mooney and R. Ewart: *Physics*, 1934, vol. 5 (11), pp. 350–54.
65. R. Whorlow: *Rheological Techniques*, E. Horwood, Chichester, 1980.
66. D. Spencer, R. Mehrabian, and M. Flemings: *Metall. Trans.*, 1972, vol. 3, pp. 1925–32.
67. M. Hashimi: *Comprehensive Materials Processing*, Elsevier, Amsterdam, 2014, vol. 1.
68. C. Jin, C. Jang, and C. Kang: *Metals*, 2015, vol. 5 (1), pp. 192–205.
69. M. Flemings, R. Riek, and K. Young: *Mater. Sci. Eng.*, 1976, vol. 25, pp. 103–17.
70. S. Ji, Z. Fan, and M. Bevis: *Mater. Sci. Eng. A*, 2001, vol. A299, pp. 210–17.
71. D. Rosato, D. Rosato, and M. Rosato: *Injection Molding Handbook*, Kluwer, Norwell, 2000.
72. V. Patel: Master Thesis, Ganpat University, India, 2014.
73. A. Olufemi and I. Ademola: *Int. J. Metall. Eng.*, 2012, vol. 1 (3), pp. 40–43.
74. M. Sauti, S. Sulamian, B. Baharudin, and M. Arifin: *Mater. Sci. Forum*, 2014, vols. 773–4, pp. 195–202.
75. R. Kumar, M. Ansari, S. Mishra, and A. Kumar: *Int. J. Eng. Res. Technol.*, 2014, vol. 3 (4), pp. 90–92.
76. S. Mishra, S. Sahu, and V. Ray: *Int. J. Technol. Res. Eng.*, 2015, vol. 3 (1), pp. 131–34.
77. Online document: *Ultra-high shear mixing and deagglomeration—Mixing Technology Insight #175*, www.mixers.com. Accessed 25 May 2016.
78. M. De Luna and Dayrit: *Proc. of The 3rd International Conference on Environmental Energy and Biotechnology*, vol. 70, pp 69–73, Singapore, 2014.
79. J. Zhang, S. Xu, and W. Li: *Chem. Eng. Process.*, 2012, vol. 57, pp. 25–41.
80. A. Pacek, S. Hall, M. Cooke, and A. Kowalski: *Emulsion Formation and Stability*, T.F. Tadros, Ed., Wiley, Weinheim, 2013.
81. J. Ross: US Patent 5,632,596, July 19, 1995.
82. E. Bosch, K. Langdon, and D. Cohen: US Patent 6,241,472, June 5, 2001.
83. F. Barailler, M. Heniche, and P. Tanguy: *Chem. Eng. Sci.*, 2006, vol. 61, p. 2888.
84. L. Doucet, G. Ascanio, and P. Tanguy: *Chem. Eng. Res. Des.*, 2005, vol. 83, p. 1186.
85. J. Tamminen and T. Koiranen: *Can. J. Chem. Eng.*, 2015, vol. 93, pp. 2245–52.
86. Z. Fan, Y. Zuo, and B. Jiang: *Mater. Sci. Forum*, 2011, vol. 690, pp. 141–44.
87. X. Zhang, H. Teng, T. Li, S. Xie, and J. Jin: *China Foundry*, 2007, vol. 4 (3), pp. 186–89.
88. B. Sivak, V. Grachev, V. Parshin, A. Chertov, S. Zarubin, V. Fisenko, and A. Solovev: *Metallurgist*, 2009, vol. 53 (7–8), pp. 469–81.
89. R. Khristinich, V. Timofeyev, V. Stafievskaya, and A. Nelenteyenko: *Molten Metal Electromagnetic Stirring in Metallurgy*, Hannover, International Scientific Colloquium Modelling for Electromagnetic Processing, 2003, pp. 29–34.
90. C. Vives: *J. Metall.*, 1998, vol. 50 (2), pp. 1–8.
91. C. Vives: WO Patent 1998030346 A1, July 16, 1998.
92. H. Kim and C. Kang: *Adv. Mater. Sci. Eng.*, 2011, Article ID 232640, pp. 1–12.
93. G. Zhu, J. Xu, Z. Zhang, Y. Bai, and L. Shi: *Acta Metall. Sin.*, 2009, vol. 22 (6), pp. 408–14.
94. I. Tzanakis, W. Xu, D. Eskin, P. Lee, and N. Kotsovinos: *Ultrason. Sonochem.*, 2015, vol. 27, pp. 72–80.

95. Online document: *Industrial Technology Program—Ultrasonic Processing of Materials Ultrasonic Processing of Materials*, US Department of Energy Office of Energy Efficiency and Renewable Energy, http://www1.eere.energy.gov. Accessed May 30, 2016.
96. W. Kong, D. Cang, and J. Song: *Metall. Mater. Trans.*, 2011, vol. 9, pp. 1844–47.
97. S. Gnapowski, Y. Tsunekawa, M. Okumiya, and K. Lenik: *Arch. Foundry Eng.*, 2013, vol. 134, pp. 39–42.
98. S. Jia and L. Nastac: *Chem. Mater. Eng.*, 2013, vol. 1 (3), pp. 69–73.
99. Online document: H. Puga, S. Costa, J. Barbosa, and C. Silva Ribeiro, *Use of Acoustic Energy in the Processing of Molten Aluminium Alloy,* http://www.repositorium.sdum.uminho.pt/. Accessed May 26, 2016.
100. S. Hua, I. Xiang, H. Zhi, and Q. Xiao: *J. Mater. Sci.*, 2011, vol. 46, pp. 3923–27.
101. Online document: A. O'Loughlin, *Effect of Argon Stirring on Inclusion Flotation Using Porous Plug, Intelligent System Center Research Symposium Spring*, Rolla, 2010, https://isc.mst.edu/. Accessed May 15, 2016.
102. P. Waite: US Patent 6,056,803 A, December 24, 1997.
103. B. Dolzenkov, V. Andreev, and V. Pimenov: US Patent 4,355,789, October 26, 1982.
104. J. Perri: US Patent 4,836,433, June 6, 1989.
105. J. Wannasin, R. Martinez, and M. Flemings: *Scripta Mater.*, 2006, vol. 55, pp. 115–18.
106. J. Wannasin, R. Martinez, and M. Flemings: *Solid State Phenom.*, 2006, vols. 116–7, pp. 366–69.
107. T. Chucheep, J. Wannasin, and S. Wisutmethagoon: *Adv. Mater. Res.*, 2014, vols. 881–3, pp. 1592–96.
108. J. Xu, G. Wu, W. Liu, Y. Zhang, and W. Ding: *J. Mag. Alloys*, 2013, vol. 1, pp. 217–23.
109. K. Young, C. Kyonka, and J. Courtois: US Patent 4,415,374, 1983.
110. J. Valle, M. Perez-Prado, and J. Bartolome: *Metall. Mater. Trans.*, 2003, vol. 44, pp. 2625–30.
111. Z. Ji, M. Hu, S. Sugiyama, and J. Yanagimoto: *Mater. Charact.*, 2008, vol. 59 (7), pp. 905–11.
112. F. Czerwinski and A. Zielinska-Lipiec: *Acta Mater.*, 2003, vol. 51 (11), pp. 3319–32.
113. T. Chen, G. Lu, Y. Ma, D. Li, and Y. Hao: *J. Alloys Compd.*, 2009, vol. 486, pp. 124–35.
114. L. Rogal, F. Czerwinski, L. Litynska-Dobrzynska, P. Bobrowski, A. Wierzbica-Miernik, and J. Dutkiewicz: *Solid State Phenom.*, 2015, vols. 217–8, pp. 381–88.
115. Y. Song, K. Park, and C. Hong: *Metall. Mater. Trans.*, 2006, vol. 47 (4), pp. 1250–56.
116. F. Czerwinski: *Acta Mater.*, 2002, vol. 50 (10), pp. 3265–81.
117. F. Czerwinski: *Metall. Mater. Trans. A*, 2002, vol. 33A, pp. 2963–72.
118. A. Luo: *Int. J. Magnesium Alloys*, 2013, vol. 1, no. 1, pp. 2–22.
119. W. Karem and K. Al-Raheem: *Int. J. Eng. Sci. Technol.*, 2011, vol. 3 (1), pp. 120–35.
120. M. Kainth and D. Gupta: *Int. J. Mech. Eng.*, 2015, vol. 2 (1), pp. 7–11.
121. S. Changjiang, H. Qingyou, and Z. Qijie: *China Foundry*, 2009, vol. 2 (2), pp. 93–103.
122. L. Pio and W. Chin: *Mater. Sci. Appl.*, 2012, vol. 3, pp. 713–18.
123. K. Sigworth and T. Kuhn: *Int. J. Metalcast.*, 2007, vol. 1 (1), pp. 31–40.
124. J. Campbell: *Int. Met. Rev.*, 1981, vol. 26, pp. 71–108.
125. J. Campbell: *Solidification Technology in the Foundry and Cast House, Proceedings of an International Conference of the Applied Metallurgy & Metals Technology Group*, Metals Society, London,1983.
126. S. Hem: *Ultrasonics*, 1967, vol. 5, pp. 202–07.
127. D. Stefanescu: *Science and Engineering of Casting Solidification*, Springer, New York, 2008.
128. J. Ferguson, B. Schultz, K. Cho, and P. Rohatgi: *Metals*, 2014, vol. 4, pp. 477–89.
129. F. Czerwinski: *Acta Mater.*, 2002, vol. 50 (10), pp. 2639–54.
130. F. Czerwinski: *Corros. Sci.*, 2014, vol. 86, pp. 1–16.
131. F. Czerwinski: *Int. Mater. Rev.*, 2015, vol. 50 (5), pp. 264–96.
132. Y. Wang, Z. Fan, and G. Thompson: *Philos. Mag.*, 2011, vol. 91 (8), pp. 516–29.
133. Online document: *EPA and NHTSA set Standards to Reduce Greenhouse Gases and Improve Fuel Economy for Model Years 2017–2025 Cars and Light Trucks*, United States Environmental Protection Agency EPA-420-F-12-051, 2012, https://www3.epa.gov. Accessed May 10, 2016.
134. S. Shaha, F. Czerwinski, W. Kasprzak, J. Friedman, and D. Chen: *Metall. Mater. Trans. A*, 2015, vol. 46A, p. 3063.
135. S. Shaha, F. Czerwinski, W. Kasprzak, J. Friedman, and D. Chen: *Metall. Mater. Trans. A*, 2016, vol. 47A, pp. 2396–409.
136. S. Shaha, F. Czerwinski, W. Kasprzak, J. Friedman, and D. Chen: *Mater. Des.*, 2015, vol. 83, pp. 801–12.
137. S. Shaha, F. Czerwinski, W. Kasprzak, J. Friedman, and D. Chen: *Int. J. Fatigue*, 2016, vol. 87, pp. 456–70.
138. S. Shaha, F. Czerwinski, W. Kasprzak, J. Friedman, and D. Chen: *Mater. Sci. Eng. A*, 2016, vol. 652, pp. 353–64.
139. F. Czerwinski: *JOM*, 2006, vol. 57 (6), pp. 17–20.
140. F. Wang, D. Eskin, T. Connolley, and J. Mi: *J. Cryst. Growth*, 2016, vol. 435, pp. 24–30.
141. D. Zhang, H. Dong, and H. Atkinson: *Metall. Mater. Trans. A*, 2016, vol. 47A, pp. 1–5.
142. F. Czerwinski and D. Kadak: US Patent 6,892,790, May 17, 2005.
143. F. Czerwinski and D. Kadak: US Patent 7,469,738 B2, December 30, 2008.
144. A. Kazakov: *Adv. Mater. Process.*, 2000, vol. 3, pp. 31–34.
145. L. Rogal, J. Dutkiewicz, H. Atkinson, L. Litynska-Dobrzynska, T. Czeppe, and M. Modigell: *Mater. Sci. Eng. A*, 2013, vol. 580A, pp. 362–73.
146. L. Rogal, J. Dutkiewicz, T. Czeppe, J. Bonarski, and B. Olszowska-Sobieraj: *Trans. Nonferrous Met. Soc. China*, 2010, vol. 20, p. S1033-6.
147. L. Rogal and J. Dutkiewicz: *Metall. Mater. Trans. A*, 2012, vol. 43A (13), pp. 5009–18.
148. S. Wu, X. Wu, and Z. Xiao: *Acta Mater.*, 2004, vol. 52, pp. 3519–24.
149. F. Czerwinski: *Acta Mater.*, 2005, vol. 53 (7), pp. 1973–84.
150. F. Czerwinski: US Patent 7,255,151, August 14, 2007.
151. F. Czerwinski: US Patent 7,237,594, July 3, 2007.
152. S. Wang, M. Zhao, Z. Ji, X. Li, Y. Wang, S. Sugiyama, and J. Yanagimoto: *Chin. J. Nonferrous Met.*, 2015, vol. 25 (6), pp. 1429–34.
153. F. Czerwinski: *Acta Mater.*, 2004, vol. 52 (17), pp. 5057–69.
154. E. Ma: *Mater. Trans.*, 2006, vol. 47 (5), pp. 1269–74.
155. D. Apelian: *Proceedings of the Army Sagamore Conference: Innovations in Materials Processing*, Eds. G.A. Bruggeman and V. Weiss, Plenum Press, New York, 1983, pp. 247–72.
156. S.T. Oktay, C.N. Chu, N. Saka, and N. Suh: *J. Eng. Ind.*, 1989, vol. 111, pp. 70–78.
157. N. Suh, N. Tsuda, M. Moon, and N. Saka: *J. Eng. Ind.*, 1982, vol. 104 (4), pp. 332–38.
158. T. Miyazaki, D. Terada, and Y. Miyajima: *J. Mater. Sci.*, 2011, vol. 46, pp. 4296–301.
159. Z. Swiatkowska-Warkocka, A. Pyatenko, F. Krok, B. Jany, and M. Marszalek: *Sci. Rep.*, 2015, vol. 5, pp. 1–6.
160. Q. Pan, S. Wiesner, and D. Apelian: *Solid State Phenom.*, 2006, vols. 116–7, pp. 402–05.
161. K. Ranier, C. Kiyan, A. Costa, and A. Simoes: *Mater. Res.*, 2012, vol. 15 (1), pp. 144–50.
162. N. Barekar, S. Tzamtzis, N. Babu, Z. Fan, and B. Dhindaw: *Metall. Mater. Trans. A*, 2009, vol. 40A, pp. 691–701.
163. F. Czerwinski: International Patent WO/2006/050599, May 18, 2006.
164. X. Liu: Ph.D. Dissertation, The University of Alabama, Tuscaloosa, Alabama, 2013.
165. L. Poovazhagan, K. Kalaichelvan, and T. Sornakumar: *Mater. Manuf. Process.*, 2016, vol. 31 (10), pp. 1275–85.
166. A. Muley: *Proceedings of 10th SARC-IRF International Conference*, New Delhi, India, 2015, pp. 24–26.
167. J. Banhart: *J. Metall.*, 2000, vol. 52 (12), pp. 22–27.
168. D. Wang and Z. Shi: *Mater. Sci. Eng. A*, 2003, vol. 361A, p. 45.
169. H. Liu, M. Xie, H. Liu, and D. Wang: *Rev. Adv. Mater. Sci.*, 2013, vol. 33, pp. 195–201.
170. A. Guner, M. Arikan, and M. Niebioglu: *Metals*, 2015, vol. 5, pp. 1553–65.

171. I. Kroupova, F. Radkovsky, P. Lichy, and V. Bednarova: *Conference Proceedings of The International Conference on Metallurgy and Materials Metall,* June 3–5, 2015, Brno, Czech Republic, 2015.
172. P. Stevenson: *Foam Engineering—Fundamentals and Applications*, Wiley, Chichester, 2012.
173. A. Greer: *Proceedings of the Solidification of Aluminum Alloys Symposium*, TMS Annual Meeting, Charlotte, NC, March 14–18, 2004.
174. F. Czerwinski, A. Zielinska-Lipiec, P. Pinet, and J. Overbeeke: *Acta Mater*., 2001, vol. 49, pp. 1225–35.
175. J. Frankland: *Plast. Tech*., 2011, vol. 8, pp. 1–4.
176. Y. Furukawa and Y. Tsunekawa: US Patent 8,992,705 B2, March 31, 2015.
177. S. Shaha, F. Czerwinski, W. Kasprzak, J. Friedman, and D. Chen: *Thermochim. Acta*, 2014, vol. 595, pp. 11–16.
178. Online document: http://www.thixomet.ru/UserFiles/File/Articles/3/15.Industrial_Application_of_Thixomet_short.pdf. Accessed July 10, 2016.
179. F. Czerwinski: *Die Cast. Eng*., 2014, vol. 58 (3), pp. 28–31.